Journal of Mathematical Biology (2024) 89:43
https://doi.org/10.1007/s00285-024-02141-5

Mathematical Biology

Optimal control of bi-seasonal hand, foot and mouth disease in mainland China suggests transmission from children and isolating older infected individuals are critical

Aili Wang[1] · Duo Bai[1,2] · Jingming He[2] · Stacey R. Smith?[3]

Received: 14 October 2023 / Revised: 22 August 2024 / Accepted: 27 August 2024 /
Published online: 27 September 2024

Abstract
Hand, foot and mouth disease (HFMD) is a Class C infectious disease that carries particularly high risk for preschool children and is a leading cause of childhood death in some countries. We mimic the periodic outbreak of HFMD over a 2-year period—with differing amplitudes—and propose a dynamic HFMD model that differentiates transmission between mature and immature individuals and uses two possible optimal-control strategies to minimize case numbers, total costs and deaths. We parameterized the model by fitting it to HFMD data in mainland China from January 2011 to December 2018, and the basic reproduction number was estimated as 0.9599. Sensitivity analysis demonstrates that transmission between immature and mature individuals contributes substantially to new infections. Increasing the isolation rates of infectious individuals—particularly mature infectious individuals—could greatly reduce the outbreak risk and potentially eradicate the disease in a relatively short time period. It follows that we have a reasonable chance of controlling HFMD if we can reduce transmission in children under 7 and isolate older infectious individuals.

Keywords HFMD · Basic reproduction number · Dynamics · Sensitivity analysis · Optimal control

Mathematics Subject Classification 92-10 · 92B99 · 49-11

✉ Aili Wang
aily_wang83@163.com

✉ Stacey R. Smith
stacey.smith@uottawa.ca

1 School of Science, Xi'an University of Technology, Xi'an 710054, People's Republic of China

2 School of Mathematics and Information Science, Baoji University of Arts and Sciences, Baoji 721013, People's Republic of China

3 Department of Mathematics and Faculty of Medicine, The University of Ottawa, Ottawa, ON K1N 6N5, Canada

1 Introduction

Hand, foot and mouth disease (HFMD)—caused by a group of enteroviruses (EVs), including Coxsackieviruses (A16), human enteroviruses (EV71) and Coxsackieviruses A4, A5 and B5—is a syndrome with a high risk of infection for preschool children (McMinn et al. 2001; Chen et al. 2010). During HFMD epidemics, kindergartens and nurseries are prone to mass infection. It was first reported in New Zealand in 1957 and was named as HFMD in the United States in 1959. The first case of HFMD in China was reported in Shanghai in 1981. Since then, HFMD has circulated throughout mainland China, Hong Kong and Taiwan (Zhao et al. 2016). In China, infectious diseases are classified into A, B, C and other infectious diseases according to the speed of transmission; the degree of harm; and the supervision, monitoring and management measures that should be undertaken. Class C infectious diseases are those that cause few deaths and have a small spread range, such as influenza, mumps and filariasis (Chinese people's net). On May 2, 2008, HFMD was classified as a Class C infectious disease in China. The HFMD case number, as well as the death toll, has always been higher than other Class C infectious diseases, such as influenza, mumps and acute hemorrhagic conjunctiva. Symptoms of HFMD include herpes in such body parts as hands, feet and mouth, fever, headache and sore throat. A few infected individuals progress to serious illness, such as myocarditis, encephalitis, meningitis and cardiomyopathy (Mathes et al. 2013). Among childhood infections in China, HFMD has the highest reported annual incidence (Yang et al. 2017) and is one of the leading causes of death in childhood infections in some countries (Yang et al. 2017; World Health Organization). A total of 2,247,241 cases and 35 deaths of HFMD in children under the age of 7 were reported in China in 2018 (Chinese Center for Disease Control).

Transmission of HFMD in mainland China exhibits complex seasonality (Xing et al. 2014; Zhao and Hu 2019; Xiao et al. 2016; Zhang et al. 2018; Wu and Gao 2020). In particular, Xiao et al. found that the incidence of both mild and severe patients decreased every 2 years, and the periodic changes of these two series could be characterized by a mixed period of 2 years, 1 year, 6 months or 8 months (Xiao et al. 2016). Since the incidence of HFMD may be a combination of many factors such as school term, large population flow during the Spring Festival, family gatherings, meteorological changes and multiple transmission routes, HFMD has complex seasonal characteristics. Wu et al. found that the annual incidence of HFMD in Xiangshan County from 2009 to 2019 and in the Fengxian District of Shanghai from 2012 to 2015 showed a clear 2-year cycle (Zhang et al. 2018; Wu and Gao 2020). Although HFMD is mainly transmitted in children under 7 years of age, it can also be transmitted in adults (Chinese Center for Disease Control and Prevention). Children are more susceptible to infection than adults because they are less likely than adults to implement self-protection measures or have proper antibodies. The spread of HFMD is heterogeneous across different age groups (Zhao et al. 2016, 2021; Xing et al. 2014; Liu et al. 2020; Li et al. 2016, 2023) and the infection rate is higher in immature individuals. In China, children stay in kindergarten for the entire day, which leads to high contact rates among these children, although their classrooms may not be crowded. It is worth emphasizing that elderly infectious individuals, along with infectious preschool children, contribute substantially to the new infections of HFMD, but few model studies focus on these populations (Qu et al.

2018; Wu et al. 2017). Efficient health interventions against HFMD are still far from adequate, so minimizing the cost of disease burden and the costs of interventions while containing the spread remains challenging.

The aim of this study is to gain insights into the transmission dynamics of HFMD by proposing a novel model incorporating two transmission paths. We will consider the differences in the transmission of HFMD within and between the immature and mature populations, mimic the bi-seasonal pattern of HFMD in mainland China and explore optimal strategies for controlling HFMD. A number of dynamic models have been proposed to understand the mechanism of HFMD transmission. Liu (2011) examined a HFMD model with periodic transmission rate qualitatively and obtained a threshold determining the extinction and uniform persistence of the disease. Ma et al. (2013) found that asymptomatic infection plays an important role in the transmission of HFMD by fitting the proposed periodic model to the HFMD data of Shandong province. Wang et al. (2016, 2019) proposed a model that included direct and indirect transmission and found that both recessive infected individuals—people infected with HFMD who are contagious but show no symptoms—and contaminated environments are important factors leading to new infections of HFMD. Shi et al. (2020) proposed a periodic model to study the impact of EV71 vaccination on the spread of multiple pathogenic viruses of HFMD in mainland China and found that the disease could be eliminated by improving protection measures and medical conditions. Dai et al. (2019) and Ding et al. (2020) established a periodic model to study the seasonal spread of HFMD in Wenzhou and found that school opening and meteorological factors were mainly responsible for the annual multiple-peak pattern of HFMD outbreaks in Wenzhou. These modelling studies investigated the seasonal infection of HFMD in mainland China qualitatively or quantitatively by incorporating periodic transmission rate with 1 year period in the targeted model. However, the number of HFMD infections in mainland China shows a periodic infection of 2 years, which has been ignored in the modelling literature thus far.

Some recent papers have used optimal control to study HFMD. Tan and Cao (2018) applied optimal-control theory to the proposed HFMD model and numerically derived an optimal-control strategy based on minimizing intervention costs and the number of infected individuals. Ding et al. (2020) studied the optimal-control strategies of a HFMD model combined with EV-A71 vaccination. By fitting the model to the HFMD reported data in Wenzhou, China, they obtained optimal-control strategies: reducing the infection rate, improving the recovery rate, paying attention to personal hygiene, reducing the contacts of infected and susceptible individuals, strengthening active treatment and enhancing immune capacity can all help control the epidemic. Wongvanich et al. (2021) applied two different optimal controls to an SEIRQ model: one with treatment only, the other with vaccination and treatment. Unsurprisingly, they found that less treatment would be required in the second option. Yang et al. (2013) also proposed an SEIRQ model, with an age cutoff at 14, using control measures for increasing social-distancing measures, decreasing the quarantine rate and treatment efforts. They applied the model to data from mainland China and determined that $R_0 > 1$ and hence the disease was persisting. Shi and Lu (2020) developed a fractional-order SEIR model for HFMD that included a compartment for environmental transmission. They found that the optimal solution was bang-bang and that treatment resulted in

less cost in the fractional-order model compared to the integer-order model. Tan et al. (2023) established a distributed lag nonlinear model with a periodic transmission rate to study the influence of external factors such as climate and environment on the transmission of HFMD. They found that several measures can be taken to control the spread of HFMD, such as early warning at the start of school. These studies focus on the optimal-control strategies of HFMD. However, few studies investigate the dynamics of bi-seasonal variations of the disease.

The organization of this paper is as follows. In the next section, we will formulate a model of HFMD. In Sect. 3, we define the basic reproduction number and investigate the global stability of disease-free equilibrium as well as the uniform persistence of the model. The parameterization and sensitivity analysis of the targeted model to the data are presented in Sect. 4. Section 5 focuses on the optimal-control strategy with two different combined objective functionals. The cases of optimal control, constant control and without control are compared numerically, and the advantages of optimal control are highlighted. We discuss the implications of our results in the final section.

2 Model formulation

HFMD was classified as a Class C Infectious Disease by the Ministry of Health of the People's Republic of China on May 2nd, 2008. Generally, healthcare workers determine whether a person is infected with HFMD by observing symptoms such as a slight fever followed by blisters and ulcers in the mouth and rashes on the hands and feet. However, confirmed results are determined in the laboratory according to samples of throat swabs or feces. The newly confirmed cases will be included by the Chinese Center for Disease Control and Prevention (China CDC) once they enter the hospital for examination (Chinese Center for Disease Control and Prevention). The confirmed data is recorded every month or year by all regions in mainland China except Hong Kong, Macao and Taiwan.

Since children are less likely to be aware of the necessity of self protection and do not have sufficient antibodies against HFMD, they are much more susceptible to the virus than adults. According to the regulations of the primary schools in China, only children over the age of 6 can be enrolled in school. Hence we divided the whole population into two subpopulations: infants or children under 7 years old and everyone else. For simplicity, we call the infants and children under 7 years old *immature* individuals and call all other individuals *mature* individuals. We have collected the data of the monthly number of new confirmed cases in infants and immature children under 7 years old from January 2011 to December 2018, as shown in Fig. 1. It follows from Fig. 1 that there exists a 2-year cycle in the data.

Based on the disease progression and the intervention measures, we extended the basic SEIR model by considering the difference of HFMD transmission among the immature population and mature population in mainland China. The total population, denoted as N, is divided into two groups: immature and mature individuals. The immature population is denoted as N_c and the mature population is denoted as N_a, with $N = N_c + N_a$. In the following, we adopted the subscript 'a' (resp., 'c') to indicate mature-related (resp., immature-related) compartments and parameters. Both N_c and

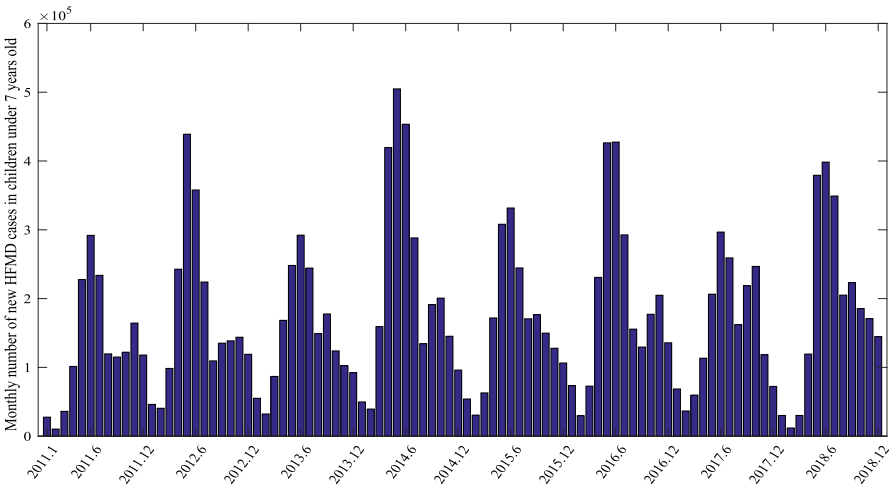

Fig. 1 The monthly number of new HFMD cases in children under 7 years old in mainland China (except Hong Kong, Macao and Taiwan) from January 2011 to December 2018

N_a are divided into five compartments: susceptible S, exposed E (infected but not infectious), infectious I (clinical or subclinical), isolated Q (hospitalized), and recovered R; i.e., $N_c = S_c+E_c+I_c+Q_c+R_c$ and $N_a = S_a+E_a+I_a+Q_a+R_a$. Susceptible individuals (S_c, S_a) may be infected by close contact with infected ones (I_c, I_a) and will enter the exposed compartment (E_c, E_a). Both the exposed immature individuals (E_c) and exposed mature individuals (E_a) are not infectious, but they will develop into infectious individuals (I_c, I_a) who may be symptomatic or asymptomatic after a latent period. If the infected individuals go to hospital for examination, they will be isolated and enter the quarantine compartment (Q_c, Q_a) until recovery (R_c, R_a) or death. Due to the short period of HFMD, we only considered the maturation of immature susceptibles and immature recovered individuals to the corresponding mature compartments in this work. In addition, there is no lifelong immunity for the recovered individuals, so we also considered immunity to be temporary. Our model is illustrated in Fig. 2. Considering that the transmission of HFMD is progressing with the unit of days, we define the parameters to be with the unit of days, although the data is in months.

Note that the data has a 2-year period and the magnitude of the second year is significantly larger than that of the first year in each period. On the one hand, Wu et al. found that the 2-year cycle may be related to the increase in population immunity after a local HFMD outbreak, with the decrease of immunity and the increase of the number of susceptibles following (Wu and Gao 2020). Zhang et al. suggested that the rise and fall of herd immunity may be responsible for the phenomenon of 2-year cycle (Zhang et al. 2018). On the other hand, we will adopt $\sigma_c E_c$ in the targeted model to fit the data on the monthly number of new immature infections in our numerical simulations. The parameter σ_c has not been considered to be periodic in existing studies, so it is reasonable to take E_c as a periodic variable with a 2-year period. Since the natural death rate is constant, it is reasonable to take the incidence rate as a 2-year periodic function. Hence we define all incidence rates as functions, which have a period of 2

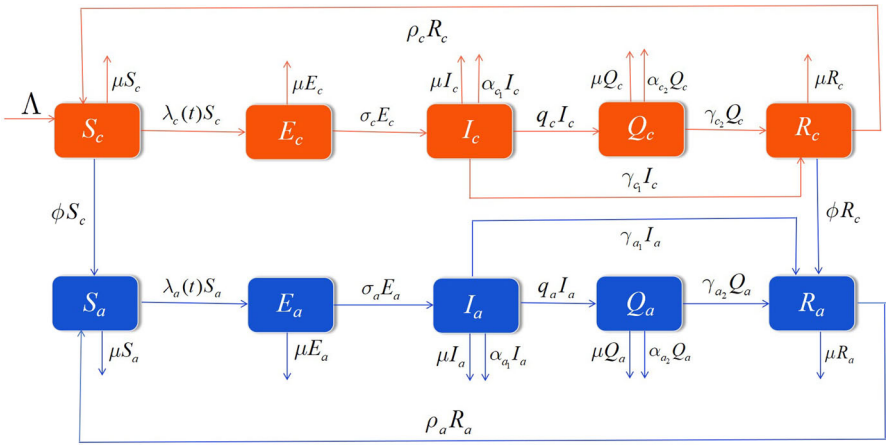

Fig. 2 A schematic flow diagram of the transmission of HFMD in mainland China with periodic transmission and quarantined

years, with a larger amplitude in year two than that in year one, as shown in Fig. 3. In Fig. 3, the function $\beta_{cc}(t)$ represents the incidence rate of immature susceptibles (S_c) after being contact with the immature infectious (I_c). The function $\beta_{ac}(t)$ represents the incidence rate of immature susceptibles (S_c) after being in contact with the mature infectious (I_a); the function $\beta_{ca}(t)$ represents the incidence rate of mature susceptibles (S_a) after being contact with the immature infectious (I_c); and the function $\beta_{aa}(t)$ represents the incidence rate of mature susceptibles (S_a) after being contact with the mature infectious (I_a). We assume the incidence rate $\beta_l(t)$, $l \in \{cc, ac, ca, aa\}$, is continuous and non-negative.

It follows from Fig. 1 that the HFMD outbreak in mainland China exhibits a cycle of 2 years with a higher peak size in the second year in each cycle. We thus construct a piecewise-defined function to mimic the bi-seasonal transmission rate. We take the transmission rate $\beta_{cc}(t)$ as an example in the following to show how these transmission functions are formulated. We initially construct a function to describe the transmission rate in the first year (denoted as T_1) of each cycle. The variation trend of the data is similar to the negative value of the sine function, so we adopt

$$-\beta_{cc2} \sin \omega(t + \theta), \tag{1}$$

where β_{cc2}, ω and θ are positive numbers. Since $\beta_{cc}(t)$ must be positive, we add a positive constant β_{cc1} to (1) to get

$$\beta_{cc1} - \beta_{cc2} \sin \omega(t + \theta), \tag{2}$$

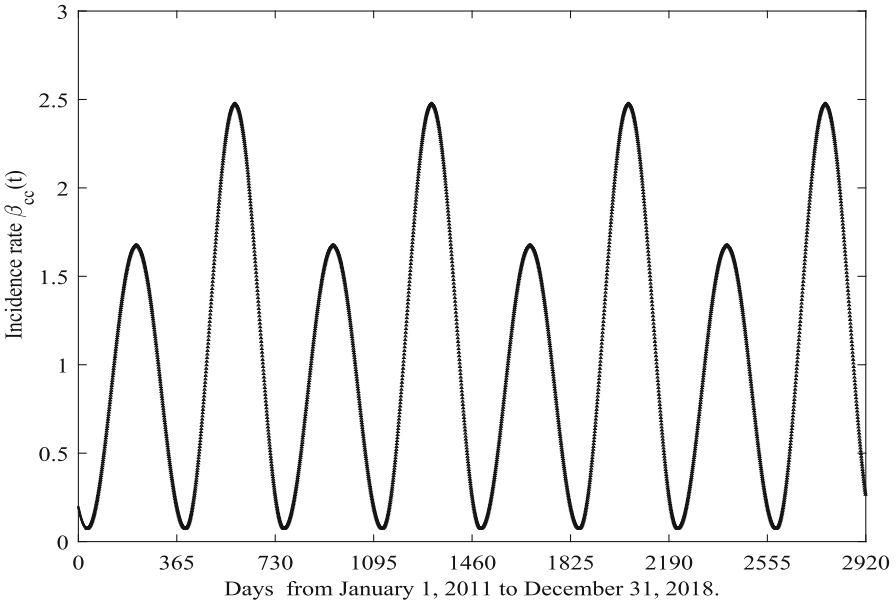

Fig. 3 Schematic diagram of the time-series plotting of the function of incidence rate $\beta_{cc}(t)$

where $\beta_{cc1} > \beta_{cc2}$. There are 365 days in a year, so $\omega = 2\pi/365$ in (2). Given that the data in the first two months of the first year of each cycle is decreasing, it is reasonable to treat it as the previous period of the sine function. Then we shift the figure of the function (2) to the left by 2 months (the first two months of each year), so $\theta = 59$ days, and the transmission rate for the first year in each cycle takes the form

$$\beta_{cc1} - \beta_{cc2} \sin \frac{2\pi}{365}(t + 59). \tag{3}$$

The transmission rate for the second year in each cycle (denoted as T_2) is similar to (3) but with a higher amplitude. We obtain from Fig. 1 that the minimum number of infections in the first and second years of each cycle is roughly equal, although their peak size is different, so we introduce parameter c_1 to ensure that the waves in each year have the same minimum but different peak values. Thus the transmission rate for the second year takes the form

$$c_1\left[\beta_{cc1} - \beta_{cc2} \sin \frac{2\pi}{365}(t + 59)\right] + (1 - c_1)(\beta_{cc1} - \beta_{cc2}). \tag{4}$$

Hence the transmission rate $\beta_{cc}(t)$ is defined as following

$$\beta_{cc}(t) = \begin{cases} \beta_{cc1} - \beta_{cc2} \sin \frac{2\pi(t+59)}{365}, & t \in T_1, \\ c_1\left[\beta_{cc1} - \beta_{cc2} \sin \frac{2\pi(t+59)}{365}\right] + (1 - c_1)(\beta_{cc1} - \beta_{cc2}), & t \in T_2, \end{cases} \tag{5}$$

where T_1 (resp., T_2) stands for the days of the first year (resp., the second year) of each cycle. If the time t falls in the first year of a cycle so that $t \in T_1$, then $\beta_{cc}(t)$ takes the form (3); otherwise, if the time t falls in the second year of a cycle so that $t \in T_2$, then $\beta_{cc}(t)$ takes the form (4). It follows that $\beta_{cc}(t)$ is bounded between $\beta_{cc1} - \beta_{cc2}$ and $\beta_{cc1} + \beta_{cc2}$.

The incidence rates $\beta_l(t)$, $l \in \{ac, ca, aa\}$, are defined as follows

$$\beta_{ac}(t) = \begin{cases} \beta_{ac1} - \beta_{ac2} \sin \frac{2\pi(t+59)}{365}, & t \in T_1, \\ c_2\left[\beta_{ac1} - \beta_{ac2} \sin \frac{2\pi(t+59)}{365}\right] + (1-c_2)(\beta_{ac1} - \beta_{ac2}), & t \in T_2. \end{cases} \tag{6}$$

$$\beta_{ca}(t) = \begin{cases} \beta_{ca1} - \beta_{ca2} \sin \frac{2\pi(t+59)}{365}, & t \in T_1, \\ c_3\left[\beta_{ca1} - \beta_{ca2} \sin \frac{2\pi(t+59)}{365}\right] + (1-c_3)(\beta_{ca1} - \beta_{ca2}), & t \in T_2, \end{cases} \tag{7}$$

$$\beta_{aa}(t) = \begin{cases} \beta_{aa1} - \beta_{aa2} \sin \frac{2\pi(t+59)}{365}, & t \in T_1, \\ c_4\left[\beta_{aa1} - \beta_{aa2} \sin \frac{2\pi(t+59)}{395}\right] + (1-c_4)(\beta_{aa1} - \beta_{aa2}), & t \in T_2. \end{cases} \tag{8}$$

It can be seen from the establishment process of formula (4) that β_{cc1} plays an important role in (4). We similarly get that β_{ac1} is a key parameter of (6). In Sect. 4.2, we will examine the effect of β_{cc1} and β_{ac1} in the spread of HFMD in mainland China. It follows that our targeted model takes the following form

$$\begin{aligned}
\frac{dS_c(t)}{dt} &= \Lambda - \lambda_c(t)S_c - \mu S_c - \phi S_c + \rho_c R_c, \\
\frac{dE_c(t)}{dt} &= \lambda_c(t)S_c - \mu E_c - \sigma_c E_c, \\
\frac{dI_c(t)}{dt} &= \sigma_c E_c - q_c I_c - \gamma_{c_1} I_c - \mu I_c - \alpha_{c_1} I_c, \\
\frac{dQ_c(t)}{dt} &= q_c I_c - \gamma_{c_2} Q_c - \mu Q_c - \alpha_{c_2} Q_c, \\
\frac{dR_c(t)}{dt} &= \gamma_{c_1} I_c + \gamma_{c_2} Q_c - \mu R_c - \phi R_c - \rho_c R_c, \\
\frac{dS_a(t)}{dt} &= \phi S_c - \mu S_a + \rho_a R_a - \lambda_a(t) S_a, \\
\frac{dE_a(t)}{dt} &= \lambda_a(t) S_a - \mu E_a - \sigma_a E_a, \\
\frac{dI_a(t)}{dt} &= \sigma_a E_a - q_a I_a - \gamma_{a_1} I_a - \mu I_a - \alpha_{a_1} I_a, \\
\frac{dQ_a(t)}{dt} &= q_a I_a - \gamma_{a_2} Q_a - \mu Q_a - \alpha_{a_2} Q_a, \\
\frac{dR_a(t)}{dt} &= \phi R_c + \gamma_{a_1} I_a + \gamma_{a_2} Q_a - \mu R_a - \rho_a R_a,
\end{aligned} \tag{9}$$

where

$$\lambda_c(t) = \frac{\beta_{cc}(t)I_c}{N_c} + \frac{\beta_{ac}(t)I_a}{N_c}, \quad \lambda_a(t) = \frac{\beta_{ca}(t)I_c}{N_a} + \frac{\beta_{aa}(t)I_a}{N_a}.$$

The detailed definitions and description of all parameters are shown in Table 1. In Sect. 4.1, we will show in detail how the least-squares method is adopted to estimate the unknown parameters.

3 Dynamic analysis

All solutions of model (9) are non-negative with non-negative initial values. In this section, we initially define the basic reproduction number of the target model based on the positiveness and ultimately boundedness of the solutions. Then we examine the global stability of the disease-free equilibrium and the existence of positive periodic solutions of model (9). To this end, we initially give the following definitions.

Definition 1 (Zhao 2003) The matrix D is *cooperative* if it has nonnegative off-diagonal entries.

Definition 2 (Huang and Yang 2007) Suppose D is a matrix of order $n(n \geq 2)$. Then matrix D is *irreducible* if there does not exist a permutation matrix P such that

$$PDP^T = \begin{bmatrix} A_{11} & A_{12} \\ 0 & A_{22} \end{bmatrix}$$

is a partitioned upper triangular matrix, where A_{11} is a square matrix of order r and A_{22} is a square matrix of order $n - r$, $1 \leq r \leq n$, and T represents the transpose of the matrix.

Denote

$$\begin{aligned} X = \big\{&(S_c, E_c, I_c, Q_c, R_c, S_a, E_a, I_a, Q_a, R_a) : S_c \geq 0, E_c \geq 0, I_c \geq 0, \\ &Q_c \geq 0, R_c \geq 0, S_a \geq 0, E_a \geq 0, I_a \geq 0, Q_a \geq 0, R_a \geq 0\big\}, \\ X_0 = \big\{&(S_c, E_c, I_c, Q_c, R_c, S_a, E_a, I_a, Q_a, R_a) \in X : E_c > 0, I_c > 0, E_a > 0, I_a > 0\big\}. \end{aligned}$$

Lemma 1 *The solutions are uniformly and ultimately bounded for system (5); i.e., there exists $t_1 > 0$, such that*

$$\begin{aligned} &(S_c(t), E_c(t), I_c(t), Q_c(t), R_c(t), S_a(t), E_a(t), I_a(t), Q_a(t), R_a(t)) \\ &\leq \left(\frac{\Lambda}{d}, \frac{\Lambda}{d}, \frac{\Lambda}{d}, \frac{\Lambda}{d}, \frac{\Lambda}{d}, \frac{\Lambda}{d}, \frac{\Lambda}{d}, \frac{\Lambda}{d}, \frac{\Lambda}{d}, \frac{\Lambda}{d}\right) \end{aligned}$$

for all $t \geq t_1$.

Table 1 Estimated initial values of variables and parameters for model (9)

Variables	Description	Initial value	Unit	Source
S_c	Immature susceptible population	102,640,976	People	Data
E_c	Immature exposed population	30,000	People	LS
I_c	Immature infectious population	20,000	People	LS
Q_c	Immature isolated population	1960	People	Calculated
R_c	Immature recovered population	3,062,932	People	Data
S_a	Mature susceptible population	1,234,016,092	People	Data
E_a	Mature exposed population	5000	People	LS
I_a	Mature infectious population	2191	People	LS
Q_a	Mature isolated population	0	People	Calculated
R_a	Mature recovered population	459,597	People	Data

Parameters	Description	Value	Unit	Resource
Λ	Birth rate of the population	43679	$\frac{\text{people}}{\text{day}}$	Calculated (National Bureau of Statistics of China)
$\beta_{cc}(t)$	Periodic transmission rate from I_c to S_c	–	–	LS
$\beta_{ac}(t)$	Periodic transmission rate from I_a to S_c	–	–	LS
$\beta_{ca}(t)$	Periodic transmission rate from I_c to S_a	–	–	LS
$\beta_{aa}(t)$	Periodic transmission rate from I_a to S_a	–	–	LS

Table 1 continued

Parameters	Description	Value	Unit	Resource
μ	Natural death rate	0.0000356	day^{-1}	Calculated (National Bureau of Statistics of China)
ϕ	Progression rate from immature population to mature population	3.9139×10^{-4}	day^{-1}	Calculated (Chinese people's net)
σ_c	Progression rate of immature exposed to infectious individuals	0.1	day^{-1}	LS
σ_a	Progression rate of mature exposed to infectious individuals	0.1	day^{-1}	LS
q_c	Isolation rate of immature infectious individuals	0.098	day^{-1}	LS
q_a	Isolation rate of mature infectious individuals	9.6424×10^{-5}	day^{-1}	LS
α_{c_1}	Disease-induced death rate of immature infectious individuals	0.4554×10^{-5}	day^{-1}	Calculated (Chinese Center for Disease Control and Prevention (China CDC))
α_{c_2}	Disease-induced death rate of immature isolated individuals Q_c	0.4554×10^{-5}	day^{-1}	Calculated (Chinese Center for Disease Control and Prevention (China CDC))
α_{a_1}	Disease-induced death rate of mature infectious individuals	0	day^{-1}	Assumed
α_{a_2}	Disease-induced death rate of mature isolated individuals	0	day^{-1}	Assumed
γ_{c_1}	Recovery rate of immature infectious individuals	0.8235/7	day^{-1}	Liu (2011)
γ_{c_2}	Recovery rate of immature isolated individuals	0.8235/7	day^{-1}	Liu (2011)
γ_{a_1}	Recovery rate of mature infectious individuals	0.8235/7	day^{-1}	Assumed
γ_{a_2}	Recovery rate of mature isolated individuals	0.8235/7	day^{-1}	Assumed
ρ_c	Remove rate of immature recovered to susceptible individuals	1.00×10^{-4}	day^{-1}	LS
ρ_a	Remove rate of mature recovered to susceptible individuals	0.0035	day^{-1}	LS

'Data' refers to the source where the values of variables can be obtained directly; 'Calculated' means that the values of the variables or parameters are calculated from the data; 'Assumed' means that the values of parameters are specified according to the assumption in fitting. LS = least squares

Proof For system (5), the total population $N(t)$ satisfies the following equation

$$N' = \Lambda - \mu N - \alpha_{c_1} I_c - \alpha_{c_2} Q_c - \alpha_{a_1} I_a - \alpha_{a_2} Q_a \leq \Lambda - \mu N,$$

so we have

$$N \leq \frac{\Lambda}{\mu} - ce^{-\mu t},$$

where c is an arbitrary constant. Hence, there exists $T > 0$ such that

$$S_j(t) \leq \frac{\Lambda}{\mu}, E_j(t) \leq \frac{\Lambda}{\mu}, I_j(t) \leq \frac{\Lambda}{\mu}, Q_j(t) \leq \frac{\Lambda}{\mu}, R_j(t) \leq \frac{\Lambda}{\mu}, j \in \{c, a\}$$

for $t \geq T$. Therefore, the solutions are uniformly and ultimately bounded. □

Lemma 2 *Both X and X_0 are positive invariant sets.*

Proof We prove that X_0 is positively invariant; the positive invariance of X can be obtained similarly. For any initial condition $\left(S_c^0, E_c^0, I_c^0, Q_c^0, R_c^0, S_a^0, E_a^0, I_a^0, Q_a^0, R_a^0\right) \in X_0$, if there is $t_1 \geq 0$ such that

$$\begin{aligned} &S_c(t_1) = 0, \quad E_c(t_1) \geq 0, \quad I_c(t_1) \geq 0, \quad Q_c(t_1) \geq 0, \quad R_c(t_1) \geq 0 \\ &S_a(t_1) \geq 0, \quad E_a(t_1) \geq 0, \quad I_a(t_1) \geq 0, \quad Q_a(t_1) \geq 0, \quad R_a(t_1) \geq 0, \end{aligned}$$

then we have $\frac{dS_c(t_1)}{dt} > 0$. Hence, we have $S_c(t) \geq 0$ for all $t \geq 0$ and so

$$\begin{aligned} E_c(t) &= e^{-(\sigma_c+\mu)t}\left[E_c^0 + \int_0^t (\lambda_c(s_1)S_c(s_1)e^{(\sigma_c+\mu)s_1}ds_1\right] \geq E_c^0 e^{-(\sigma_c+\mu)t} > 0, \\ I_c(t) &= e^{-(q_c+\gamma_{c_1}+\mu+\alpha_{c_1})t}\left[I_c^0 + \int_0^t \sigma_c E_c(s_1)e^{(q_c+\gamma_{c_1}+\mu+\alpha_{c_1})s_1}ds_1\right] \\ &\geq I_c^0 e^{-(q_c+\gamma_{c_1}+\mu+\alpha_{c_1})t} > 0, \\ Q_c(t) &= e^{-(\gamma_{c_2}+\mu+\alpha_{c_2})t}\left[Q_c^0 + \int_0^t q_c I_c(s_1)e^{(\gamma_{c_2}+\mu+\alpha_{c_2})s_1}ds_1\right] \\ &\geq Q_c^0 e^{-(\gamma_{c_2}+\mu+\alpha_{c_1})t} \geq 0, \\ R_c(t) &= e^{-(\mu+\phi+\rho_c)t}\left[R_c^0 + \int_0^t (\gamma_{c_1} I_c(s_1) + \gamma_{c_2} Q_c(s_1))e^{(\mu+\phi+\rho_c)s_1}ds_1\right] \\ &\geq R_c^0 e^{-(\mu+\phi+\rho_c)t} \geq 0 \end{aligned}$$

for all $t > 0$, where $\lambda_c(t) = \beta_{cc}(t)\frac{I_c}{N_c} + \beta_{ac}(t)\frac{I_a}{N_c}$ and $\lambda_a(t) = \beta_{ca}(t)\frac{I_c}{N_a} + \beta_{aa}(t)\frac{I_a}{N_a}$. We similarly get $S_a(t) \geq 0$, $E_a(t) > 0$, $I_a(t) > 0$, $Q_a(t) \geq 0$, $R_a(t) \geq 0$. Thus X_0 is positively invariant. □

It follows from Lemmas 1 and 2 that the set

$$\begin{aligned} X_1 \equiv \Bigg\{ & (S_c, E_c, I_c, Q_c, R_c, S_a, E_a, I_a, Q_a, R_a) : 0 \le S_c \le \frac{\Lambda}{\mu}, \\ & 0 \le E_c \le \frac{\Lambda}{\mu}, \\ & 0 \le I_c \le \frac{\Lambda}{\mu}, 0 \le Q_c \le \frac{\Lambda}{\mu}, 0 \le R_c \le \frac{\Lambda}{\mu}, \\ & 0 \le S_a \le \frac{\Lambda}{\mu}, 0 \le E_a \le \frac{\Lambda}{\mu}, 0 \le I_a \le \frac{\Lambda}{\mu}, \\ & 0 \le Q_a \le \frac{\Lambda}{\mu}, 0 \le R_a \le \frac{\Lambda}{\mu} \Bigg\} \end{aligned}$$

is positively invariant.

Let $(\mathbb{R}^n, \mathbb{R}^n_+)$ be the standard ordered n-dimensional Euclidean space with a norm $\|.\|$. For $u, v \in \mathbb{R}^n$, we denote $u \ge v$ for $u - v \in \mathbb{R}^n_+$; $u > v$ for $u - v \in \mathbb{R}^n_+ \backslash \{0\}$; $u \gg v$ for $u - v \in \text{Int}(\mathbb{R}^n_+)$. Consider $A(t)$ to be a continuous, cooperative, irreducible and periodic $n \times n$ matrix function with period $\omega > 0$. Let $\Phi_{A(.)}(t)$ be the fundamental solution matrix of the linear ordinary differential equation $x' = A(t)x$ and let $r\big(\Phi_{A(.)}(\omega)\big)$ be the spectral radius of $\Phi_{A(.)}(\omega)$. By the Perron–Frobenius theorem, $r\big(\Phi_{A(.)}(\omega)\big)$ is the principle eigenvalue of $\Phi_{A(.)}(\omega)$ in the sense that it is simple and admits an eigenvector $v^* \gg 0$.

Lemma 3 *(Zhang and Zhao 2007) There exists a positive ω-periodic function $v(t)$ such that $e^{\theta_v t} v(t)$ is a solution of the equation $x' = A(t)x$ with $\theta_v = \frac{1}{\omega} \ln r\big(\Phi_{A(.)}(\omega)\big)$, where the matrix $A(t)$ is continuous, cooperative and irreducible.*

We next define the basic reproduction number R_0 of model (9) by the result in Wang and Zhao (2008). The compartments related to new infections for model (9) are E_c, I_c, E_a, I_a, so the relevant differential equations are

$$\begin{aligned} \frac{dE_c(t)}{dt} &= \frac{\beta_{cc}(t) S_c I_c}{N_c} + \frac{\beta_{ac}(t) S_c I_a}{N_c} - \mu E_c - \sigma_c E_c, \\ \frac{dI_c(t)}{dt} &= \sigma_c E_c - q_c I_c - \gamma_{c_1} I_c - \mu I_c - \alpha_{c_1} I_c, \\ \frac{dE_a(t)}{dt} &= \frac{\beta_{ca}(t) S_a I_c}{N_a} + \frac{\beta_{aa}(t) S_a I_a}{N_a} - \mu E_a - \sigma_a E_a, \\ \frac{dI_a(t)}{dt} &= \sigma_a E_a - q_a I_a - \gamma_{a_1} I_a - \mu I_a - \alpha_{a_1} I_a. \end{aligned} \tag{10}$$

Denote $Z = (E_c(t), I_c(t), E_a(t), I_a(t))$ so that $\dot{Z} = G(Z)$. Let $G(Z) = \mathscr{F} - \mathscr{V}$, where $\mathscr{F}$ represents the vector of new infections and $\mathscr{V}$ represents the vector of all other transitions. We have

$$\mathscr{F} = \begin{bmatrix} \frac{\beta_{cc}(t)S_cI_c}{N_c} + \frac{\beta_{ac}(t)S_cI_a}{N_c} \\ 0 \\ \frac{\beta_{ca}(t)S_aI_c}{N_a} + \frac{\beta_{aa}(t)S_aI_a}{N_a} \\ 0 \end{bmatrix},$$

$$\mathscr{V} = \begin{bmatrix} (\sigma_c + \mu)E_c \\ -\sigma_c E_c + \big(q_c + \gamma_{c_1} + \mu + \alpha_{c_1}\big)I_c \\ (\sigma_a + \mu)E_a \\ -\sigma_a E_a + \big(q_a + \gamma_{a_1} + \mu + \alpha_{a_1}\big)I_a \end{bmatrix}.$$

Differentiating $\mathscr{F}$ and $\mathscr{V}$ with respect to Z and computing them at the disease-free equilibrium gives

$$F(t) = \begin{bmatrix} 0 & \beta_{cc}(t) & 0 & \beta_{ac}(t) \\ 0 & 0 & 0 & 0 \\ 0 & \beta_{ca}(t) & 0 & \beta_{aa}(t) \\ 0 & 0 & 0 & 0 \end{bmatrix},$$

$$V(t) = \begin{bmatrix} \sigma_c + \mu & 0 & 0 & 0 \\ -\sigma_c & q_c + \gamma_{c_1} + \mu + \alpha_{c_1} & 0 & 0 \\ 0 & 0 & \sigma_a + \mu & 0 \\ 0 & 0 & -\sigma_a & q_a + \gamma_{a_1} + \mu + \alpha_{a_1} \end{bmatrix}.$$

Linearizing model (9) at the disease-free equilibrium $E_0\big(\frac{\Lambda}{\phi+\mu}, 0, 0, 0, 0, \frac{\Lambda\phi}{\mu(\phi+\mu)}, 0, 0, 0, 0\big)$ gives the following four-dimensional equations:

$$\begin{aligned} \frac{dE_c(t)}{dt} &= \beta_{cc}(t)I_c + \beta_{ac}(t)I_a - \mu E_c - \sigma_c E_c, \\ \frac{dI_c(t)}{dt} &= \sigma_c E_c - q_c I_c - \gamma_{c_1} I_c - \mu I_c - \alpha_{c_1} I_c, \\ \frac{dE_a(t)}{dt} &= \beta_{ca}(t)I_c + \beta_{aa}(t)I_a - \mu E_a - \sigma_a E_a, \\ \frac{dI_a(t)}{dt} &= \sigma_a E_a - q_a I_a - \gamma_{a_1} I_a - \mu I_a - \alpha_{a_1} I_a, \end{aligned} \tag{11}$$

which is equivalent to $\frac{dZ}{dt} = (F(t) - V(t))Z$.

For the linear periodic system

$$\frac{dx}{dt} = -V(t)x,$$

suppose that $X(t, s), t \geq s$ is the evolutionary operator in the system (i.e., $\frac{dX(t,s)}{dt} = -V(t)X(t, s)$ for all $t \geq s$) and satisfies $X(s, s) = \boldsymbol{I}$, where $\boldsymbol{I}$ is the 4×4 identity matrix. Let C_ω be the ordered Banach space of all ω-periodic functions from $\mathbb{R}$ to $\mathbb{R}^4$. Denote the positive cone

$$C_\omega^+ = \left\{\psi \in C_\omega : \psi(t) \geq 0, \text{for all } t \in \mathbb{R}\right\}$$

where C_ω^+ is equipped with the maximum norm $\|.\|$. Denote the initial distribution of the first infectious individuals in the periodic environment as $\psi(s) \in C_\omega$, so the distribution of the new infections resulting from infected individuals introduced at time s is $F(s)\psi(s)$, and $X(t,s)F(s)\psi(s)$ is the distribution of those new infections at time s that are still in the infectious compartments at time t for $t \geq s$. Thus

$$\phi(t) \equiv \int_{-\infty}^{t} X(t,s)F(s)\psi(s)ds = \int_0^{\infty} X(t,t-a)F(t-a)\psi(t-a)da$$

is the distribution of the total new infections at time t resulting from those infectious individuals $\psi(s)$ introduced before t.

Following Jing et al. (2020), define the linear operator $L : C_\omega \to C_\omega$ as follows:

$$(L\psi)(t) = \int_0^{\infty} X(t,t-a)F(t-a)\psi(t-a)da, \psi \in C_\omega$$

for all $t \in \mathbb{R}$. For the periodic epidemic model (9), the basic reproduction number is the spectral radius of L; i.e.,

$$R_0 = r(L). \tag{12}$$

Formula (12) provides an implicit expression of the basic reproduction number R_0, which depends on many parameters, such as the transmission rates $\beta_{cc}(t)$, $\beta_{ac}(t)$, $\beta_{ca}(t)$, $\beta_{aa}(t)$, the isolation rates q_c, q_a and so on. It will be computed numerically in Sect. 4.1.

For the following linear ω-periodic system

$$\frac{dy}{dt} = \left(-V(t) + \frac{F(t)}{\lambda}\right) y, \ t \in \mathbb{R}, \tag{13}$$

let $Y(t,\lambda)$ be the monodromy matrix with $\lambda \in (0,\infty)$. It is easy to prove that $F(t)$ is non-negative and $-V(t)$ is cooperative, so $r(Y(\omega,\lambda))$ is continuous and nonincreasing for $\lambda \in (0,\infty)$ and $\lim_{\lambda\to 0} r(Y(\omega,\lambda)) < 1$. According to Wang and Zhao (2008), it is not difficult to prove that model (9) satisfies conditions $A(1)$–$A(7)$. Then we get the following conclusion.

Lemma 4 (Wang and Zhao 2008, Theorem 2.1) *For system (9), we have:*

(i) *If there exists one positive solution λ_0 for $r(Y(\omega,\lambda)) = 1$, then λ_0 is an eigenvalue of L, so $R_0 > 0$.*
(ii) *If $R_0 > 0$, then $\lambda = R_0$ is the unique solution of $r(Y(\omega,\lambda)) = 1$.*
(iii) *$R_0 = 0$ if and only if $r(Y(\omega,\lambda)) < 1$ for all $\lambda > 0$.*

Let $Y(t, s, \lambda), t \geq s$ be the evolution operator of system (13) on $\mathbb{R}^4$. Clearly, $\Phi_{F-V}(t) = Y(t, 0, 1), t \geq 0$. Hence, we derive

$$\Phi_{F/\lambda-V}(t) = Y(t, 0, \lambda). \tag{14}$$

It follows from Lemma 4 that the basic reproduction number R_0 is the unique solution of the equation with respect to λ; i.e., $r(Y(\omega, 0, \lambda)) = 1$. The next result is from Wang and Zhao (2008).

Lemma 5 *For system (9), we have:*

(i) $R_0 = 1$ *if and only if* $r(\Phi_{F-V}(\omega)) = 1$;
(ii) $R_0 > 1$ *if and only if* $r(\Phi_{F-V}(\omega)) > 1$;
(iii) $R_0 < 1$ *if and only if* $r(\Phi_{F-V}(\omega)) < 1$.

When $R_0 < 1$, E_0 is locally asymptotically stable, whereas E_0 is unstable if $R_0 > 1$.

Next, we investigate the global stability of E_0. Let $f : X \to X$ be a continuous map and

$$\partial X_0 \equiv X \backslash X_0, \quad M_\partial \equiv \left\{ x \in \partial X_0 : f^n(x) \in \partial X_0, n \geq 0 \right\}.$$

Suppose that there exists a maximal compact invariant set A_∂ of f in ∂X_0. If there exists a Morse decomposition $\mathscr{M} \equiv \{M_1, M_2, ..., M_k\}$ of A_∂, then $\mathscr{M}$ is an acyclic covering of $\Omega(M_\partial)$, where $\mathscr{M}$ is a finite sequence of disjoint, compact, invariant and isolated subsets of ∂X_0, $\Omega(M_\partial) \equiv \bigcup_{x \in M_\partial} \omega(x)$ and $\omega(x)$ represents the omega limit set of x. We initially present the following persistence theory from Zhao (2003) for the convenience of our following proof.

Lemma 6 *Assume that*

(C_1) $f(X_0) \subset X_0$ *and there is a global attractor* A *for* f;
(C_2) *The maximal compact invariant set* $A_\partial = A \cap M_\partial$ *of* f *in* ∂X_0, *possibly empty, admits a Morse decomposition* $\{M_1, M_2, ..., M_k\}$ *with the following properties: (a)* M_i *is isolated in* X; *(b)* $W^s(M_i) \cap X_0 = \emptyset$ *for each* $1 \leq i \leq k$, *where* $W^s(M_i) = \{x \in X : \lim_{n \to \infty} d(f^n(x), M_i) = 0\}$ *represents the stable set of* M_i, $d(x, M_i) \equiv \inf_{y \in M_i} d(x, y)$.

Then there exists a $\delta > 0$ *such that for any compact internally chain transitive set* L *with* $L \nsubseteq M_i$ *for all* $1 \leq i \leq k$, *we have* $\inf_{x \in L} d(x, \partial X_0) > \delta$; *that is,* $f : X \to X$ *is uniformly persistent with respect to* $(X_0, \partial X_0)$.

Theorem 1 *If* $R_0 < 1$, E_0 *is globally asymptotically stable, whereas* E_0 *is unstable if* $R_0 > 1$.

Proof According to Lemma 5, E_0 is locally asymptotically stable for $R_0 < 1$. So we only need to prove that E_0 is globally attractive. Since $\frac{S_c}{N_c} \leq \frac{S_c}{S_c} = 1$ and $\frac{S_a}{N_a} \leq \frac{S_a}{S_a} = 1$, we have the following inequalities

$$\frac{dE_c(t)}{dt} \leq \beta_{cc}(t) I_c + \beta_{ac}(t) I_a - \mu E_c - \sigma_c E_c,$$

$$\begin{aligned}
\frac{dI_c(t)}{dt} &= \sigma_c E_c - q_c I_c - \gamma_{c_1} I_c - \mu I_c - \alpha_{c_1} I_c,\\
\frac{dE_a(t)}{dt} &\le \beta_{ca}(t) I_c + \beta_{aa}(t) I_a - \mu E_a - \sigma_a E_a,\\
\frac{dI_a(t)}{dt} &= \sigma_a E_a - q_a I_a - \gamma_{a_1} I_a - \mu I_a - \alpha_{a_1} I_a.
\end{aligned}$$

Consider the following auxiliary system:

$$\begin{aligned}
\frac{dm_1}{dt} &= \beta_{cc}(t) m_2 + \beta_{ac}(t) m_4 - (\mu + \sigma_c) m_1,\\
\frac{dm_2}{dt} &= \sigma_c m_1 - (q_c + \gamma_{c_1} + \mu + \alpha_{c_1}) m_2,\\
\frac{dm_3}{dt} &= \beta_{ca}(t) m_2 + \beta_{aa}(t) m_4 - (\mu + \sigma_a) m_3,\\
\frac{dm_4}{dt} &= \sigma_a m_3 - (q_a + \gamma_{a_1} + \mu + \alpha_{a_1}) m_4.
\end{aligned} \tag{15}$$

Denote

$$A(t) = \begin{bmatrix}
-(\sigma_c + \mu) & \beta_{cc}(t) & 0 & \beta_{ac}(t)\\
\sigma_c & -(q_c + \gamma_{c_1} + \mu + \alpha_{c_1}) & 0 & 0\\
0 & \beta_{ca}(t) & -(\sigma_a + \mu) & \beta_{aa}(t)\\
0 & 0 & \sigma_a & -(q_a + \gamma_{a_1} + \mu + \alpha_{a_1})
\end{bmatrix},$$

and note that $A(t)$ is continuous since $\beta_{cc}(t)$, $\beta_{ac}(t)$, $\beta_{ca}(t)$ and $\beta_{aa}(t)$ are continuous. We further know that $A(t)$ is cooperative according to Definition 2.1. Then we claim $A(t)$ is irreducible. In fact, for the permutation matrix

$$B = \begin{bmatrix}
0 & 0 & 1 & 0\\
1 & 0 & 0 & 0\\
0 & 1 & 0 & 0\\
0 & 0 & 0 & 1
\end{bmatrix},$$

direct calculation yields that

$$BA(t)B^T = \begin{bmatrix}
0 & 0 & 1 & 0\\
1 & 0 & 0 & 0\\
0 & 1 & 0 & 0\\
0 & 0 & 0 & 1
\end{bmatrix} \times$$

$$\begin{bmatrix}
-(\sigma_c + \mu) & \beta_{cc}(t) & 0 & \beta_{ac}(t)\\
\sigma_c & -(q_c + \gamma_{c_1} + \mu + \alpha_{c_1}) & 0 & 0\\
0 & \beta_{ca}(t) & -(\sigma_a + \mu) & \beta_{aa}(t)\\
0 & 0 & \sigma_a & -(q_a + \gamma_{a_1} + \mu + \alpha_{a_1})
\end{bmatrix} \times$$

$$\begin{bmatrix} 0 & 1 & 0 & 0 \\ 0 & 0 & 1 & 0 \\ 1 & 0 & 0 & 0 \\ 0 & 0 & 0 & 1 \end{bmatrix}$$

$$= \begin{bmatrix} -(\sigma_a+\mu) & 0 & \beta_{ca}(t) & \beta_{aa}(t) \\ 0 & -(\sigma_c+\mu) & \beta_{cc}(t) & \beta_{ac}(t) \\ 0 & \sigma_c & -(q_c+\mu+\alpha_{c_1}+\gamma_{c_1}) & 0 \\ \sigma_a & 0 & 0 & -(q_a+\mu+\alpha_{a_1}+\gamma_{a_1}) \end{bmatrix}$$

is not a block upper triangular matrix. Similarly, for any permutation matrix B, $BA(t)B^T$ is not a block upper triangular matrix. Thus, by Lemma 3, there exists a positive ω-periodic function $m(t) = (m_1(t), m_2(t), m_3(t), m_4(t))$ such that $e^{\theta_1 t}m(t)$ is a solution of system (15), where $\theta_1 = \frac{1}{\omega}\ln r(\Phi_A(\omega))$. Note that $A(t) = F(t) - V(t)$, so $\theta_1 = \frac{1}{\omega}\ln r\big(\Phi_{F-V}(\omega)\big)$. By the comparison theorem, we have $J(t) \le e^{\theta_1 t}m(t)$, where $J(t) = \big(E_c(t), I_c(t), E_a(t), I_a(t)\big)^T$ and T represents the transpose of the matrix. By Lemma 5, if $R_0 < 1$, then $r\big(\Phi_{F-V}(\omega)\big) < 1$, so $\theta_1 < 0$. Hence, we have

$$\lim_{t\to\infty} E_c(t) = 0, \lim_{t\to\infty} I_c(t) = 0, \lim_{t\to\infty} E_a(t) = 0, \lim_{t\to\infty} I_a(t) = 0.$$

Substituting into system (9), we obtain

$$\frac{dQ_c}{dt} < 0, \frac{dR_c}{dt} < 0, \frac{dQ_a}{dt} < 0, \frac{dR_a}{dt} < 0,$$

so

$$\lim_{t\to\infty} Q_c(t) = 0, \lim_{t\to\infty} R_c(t) = 0, \lim_{t\to\infty} Q_a(t) = 0, \lim_{t\to\infty} R_a(t) = 0.$$

For the first and sixth equation of system (9), we have

$$\lim_{t\to\infty} S_c(t) = \frac{\Lambda}{\phi+\mu}, \lim_{t\to\infty} S_a(t) = \frac{\Lambda\phi}{\mu(\phi+\mu)}.$$

Thus, E_0 is globally attractive for $R_0 < 1$, and so E_0 is globally asymptotically stable. □

Theorem 2 *When $R_0 > 1$, there is at least one positive periodic solution for model (9).*

See Appendix A for proof.

4 Numerical simulations

4.1 Parameter estimation and model fitting

In this section, we estimate the initial conditions and the values for all parameters. The initial conditions for the variables S_c, R_c, S_a, R_a can be obtained directly from the

data. The initial values of Q_c and Q_a as well as values of the parameters Λ, μ, ϕ, α_{c1} and α_{c2} will be calculated from the data. The values of the parameters γ_{c1} and γ_{c2} are taken from the literature. The values of the parameters $\alpha_{a1}, \alpha_{a2}, \gamma_{a1}$ and γ_{a2} will be assumed based on the transmission of HFMD in mainland China. The initial conditions of the other variables as well as the values of the other parameters will be estimated using our targeted model (9).

The surveillance system provides data on HFMD cases in mainland China every month. To fit our targeted model (9) to the data, we initially analyze the data to set the initial values for the state variables; i.e., the value of the state variables in 2011. According to the 7th census of the National Bureau of Statistics of China, the total population in 2010 was 1,339,720,000 (National Bureau of Statistics of China). Note that the number of children under 7 years old accounted for approximately 7.89% of the total population, so we derive the number of mature susceptible individuals in 2011 to be $S_a(0) = 1{,}339{,}720{,}000 \times (1 - 7.89\%) = 1{,}234{,}016{,}092$. We determine the number of immature recovered individuals by calculating the total number of immature individuals who were infected before 2011 and still less than 7 years old in 2011; i.e., $R_c(0) = 3{,}062{,}932$. The number of immature susceptible individuals in 2011 is then $S_c(0) = 102{,}640{,}976$. We similarly calculate the number of mature recovered individuals in 2011 as $R_a(0) = 459{,}597$. When the number of immature infectious individuals (I_c) and the isolation rate of I_c (i.e., q_c) are estimated, we can calculate the number of immature isolated individuals as following $Q_c = q_c \times I_c$, and we can similarly calculate the number of mature isolated individuals Q_a. We obtain the annual birth rate, calculate the average and divide it by 365 to get the recruitment rate of susceptible individuals per day, $\Lambda = 43{,}679$. Assume that the average life span of the population is 77 years, we calculate the natural death rate as $\mu = 3.56 \times 10^{-5}$. Since we have defined the population under the age of 7 as the immature infected population, the progression rate from immature population to mature population is $\phi = 3.9139 \times 10^{-4}$. We calculate the ratio of the disease-induced deaths to the case number per month from 2011 to 2018 and average it to obtain the disease-induced death rate of the immature individuals, i.e., $\alpha_{c1} = \alpha_{c2} = 0.4554 \times 10^{-5}$. Since the death among the mature infecteds is rare, we assume the disease-induced death rate of the mature individuals is $\alpha_{a1} = \alpha_{a2} = 0$. For simplicity, we assume the recovery rates of mature infectious and isolated individuals (i.e., γ_{a1} and γ_{a2}) are equal to the recovery rates of immature infectious and isolated individuals (i.e., γ_{c1} and γ_{c2}). The data we used for fitting is relatively limited, so we make this assumption although in truth the antibodies in mature individuals would likely lead to a relatively higher recovery rate. All the other parameters were estimated or from the references.

We next conducted data fitting using our targeted model to estimate the values of the parameters. There are generally three parameter-estimation methods: least squares, maximum likelihood estimation, and Bayesian estimation of which the least-squares method is easiest, minimizing the sum of squares of errors between the simulated and the actual data (Johnson and Faunt 1992). The objective function is

$$f(\Theta) = \sum_{k=1}^{k=n} (\widetilde{C}(T_k) - C(T_k))^2,$$

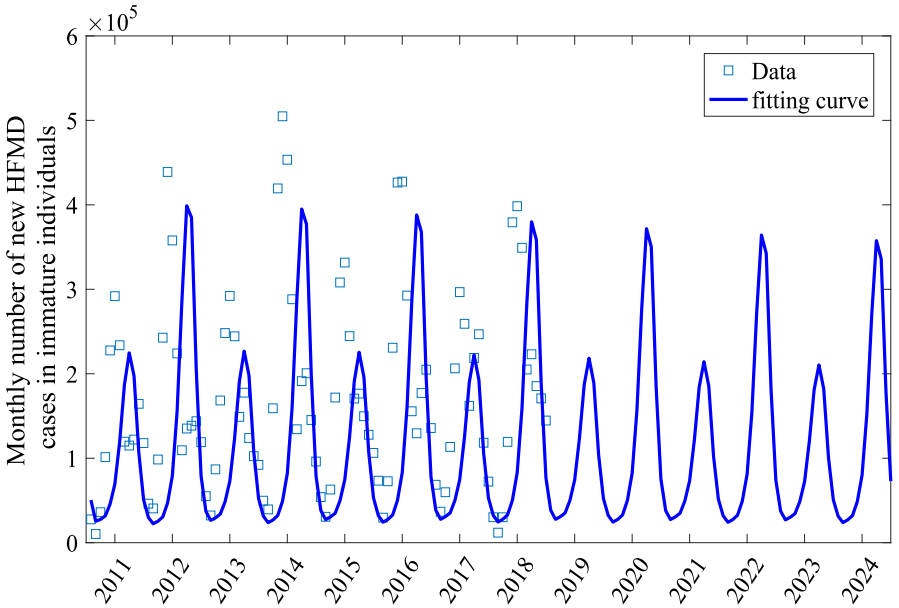

Fig. 4 Fitting result for the data on the monthly number of new HFMD cases in immature individuals in mainland China from January 2011 to December 2018

where Θ is the vector of parameters to be estimated and n is the length of the epidemic data. Here $n = 96$, since we used data from January 2011 to December 2018, lasting for 96 months. T_k is the corresponding month of the k-th month from January 2011 to December 2018. $\widetilde{C}(T_k)$ represents the actual monthly number of HFMD cases on date T_k, and $C(T_k)$ is the estimated monthly number of HFMD cases on the date T_k. In China, once immature individuals are infected with HFMD, almost all of them will go to the hospital for treatment, which results in them being recorded by China's CDC, so the data used for fitting is that of newly infected immature individuals. Thus the dynamics of $C(t)$ are governed by

$$C(t) = \sigma_c E_c.$$

By fitting our targeted model to the HFMD data on the monthly number of new cases from January 2011 to December 2018, we obtained estimates of all unknown parameters. For parameter fitting, we adjust the value ranges of the parameters to be estimated and apply multiple restarts with our least-squares approach. Using the approximate degree of the fitting curve, we obtained a satisfactory fitting result of model (9) to the HFMD data, as shown in Fig. 4. In Fig. 4, the thin blue boxes represent the monthly number of new HFMD cases in mainland China from January 2011 to December 2018, and the best fitting curve is represented by a dark blue solid line, indicating that our target model captures the data well. The estimated values for the unknown parameters and initial conditions for the variables were reported in Table 1. The incidence rate were estimated as follows:

$$\beta_{cc}(t) = \begin{cases} 1.1800 \times 10^{-1} - 1.1400 \times 10^{-1} \sin \dfrac{2\pi(t+59)}{365}, & t \in T_1, \\ 1.1400\left[1.1800 \times 10^{-1} - 1.1400 \times 10^{-1} \sin \dfrac{2\pi(t+59)}{365}\right] - 5.6000 \times 10^{-4}, & t \in T_2. \end{cases}$$

$$\beta_{ac}(t) = \begin{cases} 3.0400 \times 10^{-1} - 2.3500 \times 10^{-2} \sin \dfrac{2\pi(t+59)}{365}, & t \in T_1, \\ 1.1505\left[3.0400 \times 10^{-1} - 2.3500 \times 10^{-2} \sin \dfrac{2\pi(t+59)}{365}\right] - 4.2220 \times 10^{-2}, & t \in T_2. \end{cases}$$

$$\beta_{ca}(t) = \begin{cases} 3.1486 \times 10^{-4} - 1.0000 \times 10^{-5} \sin \dfrac{2\pi(t+59)}{365}, & t \in T_1, \\ 1.5000\left[3.1486 \times 10^{-4} - 1.0000 \times 10^{-5} \sin \dfrac{2\pi(t+59)}{365}\right] - 1.5000 \times 10^{-4}, & t \in T_2, \end{cases}$$

$$\beta_{aa}(t) = \begin{cases} 1.1585 \times 10^{-1} - 4.0000 \times 10^{-3} \sin \dfrac{2\pi(t+59)}{365}, & t \in T_1, \\ 1.2001\left[1.1585 \times 10^{-1} - 4.0000 \times 10^{-3} \sin \dfrac{2\pi(t+59)}{365}\right] - 2.2380 \times 10^{-2}, & t \in T_2. \end{cases}$$

It should be noted that the data on the monthly number of new cases we used to fit the model are not very regular in periodicity, and there are a few outliers. In addition, in order to improve the stability of the parameter estimates used in this work, we selected a relatively large amount of 8-year real data; i.e., 96 months of data, for fitting. Parameter estimation for our model is difficult: there are many parameters that need to be estimated, and the periodic incidence rates are complex and time dependent, which increases the difficulty of parameter estimation. In addition, multi-year data on HFMD cases are fitted simultaneously, and the high dimensionality and nonlinearity of the target model (5) and the standard incidence rates are different, which also increases the difficulty of parameter estimation. In fact, all the issues—including the high dimensionality and nonlinearity of the target model, the large amount of data, the time dependence and nonlinearity of many parameters—mean that running once takes a long time, occupying large computer memory, so it is not easy to find relatively good fitting results. However, we provide a qualitatively acceptable visual fit, as shown in Fig. 4. In addition, with these parameter values, we can estimate the basic reproduction number $R_0 = 0.9599 < 1$, which is only slightly below the threshold, so it is unlikely that HFMD will go extinct any time soon. In addition, we also calculated the effective reproduction number R_t from 2011 to 2018 and found that R_t is not always less than 1 but is greater than 1 during the annual HFMD epidemic, as shown in Fig. 5. The light gray bars represent the data on the number of immature infections in China from 2011 to 2018, and the yellow solid curve represents the effective reproduction number R_t. The effective reproduction number R_t is obtained by using the next-generation method, and it takes the form $R_t = \frac{a+b+c}{2}$, where

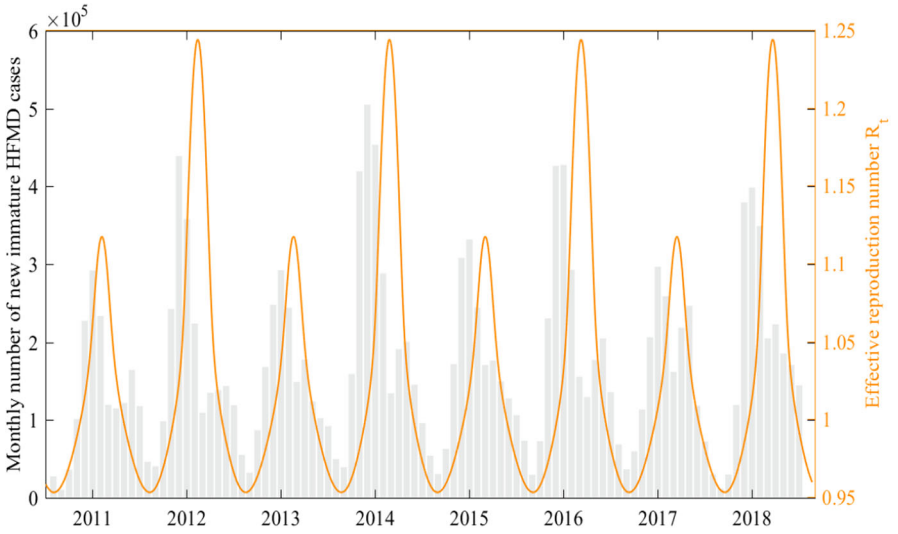

Fig. 5 Effective reproduction number R_t from January 2011 to December 2018

$$a = \frac{\sigma_c \beta_{cc}(t)}{(\sigma_c + d)(q_c + d + \gamma_{c1} + \gamma_{c2})}, \quad b = \frac{\sigma_a \beta_{aa}(t)}{(\sigma_a + d)(q_a + d + \gamma_{a1} + \gamma_{a2})},$$
$$c = \sqrt{(a-b)^2 + 4ef},$$
$$e = \frac{\sigma_a \beta_{ac}(t)}{(\sigma_a + d)(q_a + d + \gamma_{a1} + \gamma_{a2})}, \quad f = \frac{\sigma_c(t) \beta_{ca}(t)}{(\sigma_c + d)(q_c + d + \gamma_{c1} + \gamma_{c2})}.$$

To further illustrate statistically that the incidence with the 2-year cycle can fit the data better than the incidence with the 1-year cycle, we also adopt the latter incidence to fit the data. The details are in the Appendix E. The AIC value of the model with a 1-year period is 2342.6, which is 7.09% greater than 2326.1, the AIC value of the model with a 2-year period, justifying our choice of a 2-year transmission rate period.

4.2 Sensitivity analysis

In order to study the effect of hygiene-prevention measures (such as hand washing, irregular cleaning and disinfection of frequently touched surfaces, etc.), enhanced media reporting, timely hospitalization and enhanced viral-load-detection technologies in containing the HFMD spread in mainland China, we explore the impact of periodic transmission rates between immature infectious and susceptible individuals (i.e., $\beta_{cc2}(t)$) or between mature infectious and immature susceptible individuals (i.e., $\beta_{ac2}(t)$); the isolation rate of immature infectious individuals (i.e., q_c); and the progression rate from immature exposed to infectious individuals (i.e., σ_c). If the protective measures are relaxed or the control measures are strengthened, the contact rate

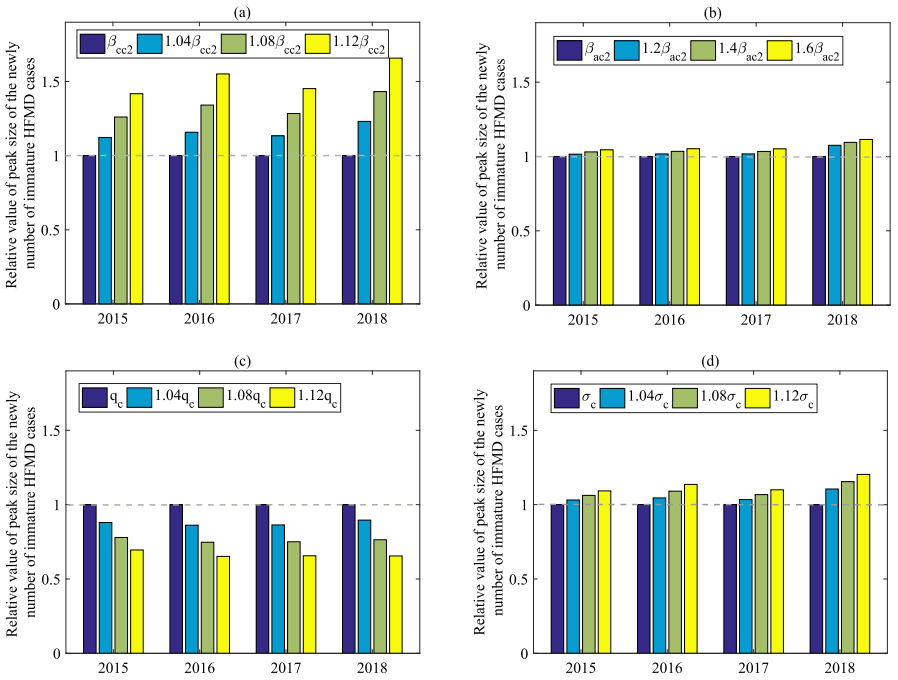

Fig. 6 Relative changes in peak size of the newly number of immature HFMD cases as **a** $\beta_{cc2}(t)$ is increased by 4%, 8% and 12%, **b** $\beta_{ac2}(t)$ is increased by 20%, 40% and 60%, **c** q_c is raised by 4%, 8% and 12%, and **d** σ_c is increased by 4%, 8% and 12%, of its baseline value. Other parameters are given in Table 1. The grey dashed lines indicate the value 1

between immature individuals ($\beta_{cc2}(t)$) or the isolation rate of immature infecteds (q_c) increases; if the viral load detection of HFMD is improved, the incubation period ($1/\sigma_c$) decreases. We assume that β_{cc}, q_c and σ_c increase by 4%, 8% and 12%, respectively, from the baseline. Once the measures are relaxed, contacts between adults would increase significantly because they need to go out for work. Moreover, they do not pay enough attention to HFMD, since it is a disease mainly transmitted among immature individuals, so we assume that the variation in the transmission from the mature infectious individuals is greater. In our simulations, we assume the transmission rate from mature infectious individuals to immature susceptibles (i.e., β_{ac2}) increases by 20%, 40% and 60% from the baseline value. The subsequent analysis shows that the number of new infections is not sensitive to the parameter β_{ac2}, which further supports the selection of a larger factor for β_{ac2}. We thus conducted a sensitivity analysis based on the above variation to show what would happen, as illustrated in Figs. 6 and 7. In Figs. 6 and 7, the baseline value 1 refers to the outcome based on the parameter values reported in Table 1; relative values in Fig. 6 (resp., Fig. 7) represent the ratios of the peak sizes (resp., cumulative number) of new infections in 2017–2018 to the baseline values. Figures 6a and 7a show that a small increase in the transmission rate from immature infectious to susceptible individuals would lead to a large increase in new infections, demonstrating that the incidence of HFMD cases is very sensitive

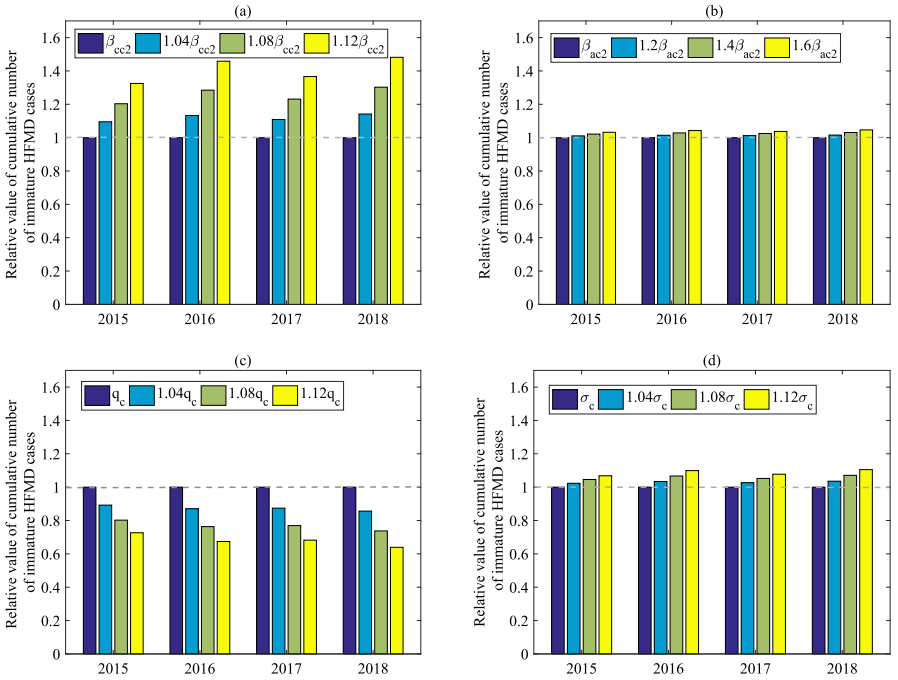

Fig. 7 Relative changes in the cumulative number of immature HFMD cases as **a** $\beta_{cc2}(t)$ is increased by 4%, 8% and 12%, **b** $\beta_{ac2}(t)$ is increased by 20%, 40% and 60%, **c** q_c is raised by 4%, 8% and 12%, and **d** σ_c is increased by 4%, 8% and 12%, of its baseline value. Other parameters are given in Table 1. The grey dashed lines indicate the value 1

to the transmission rate between immature infectious and susceptible individuals. In fact, a 12% increase in parameter β_{cc2} leads to a 57.04% and 43.52% increase in the peak size and cumulative number of infections in 2017–2018, respectively. Figures 6b and 7b show that a large change in the transmission rate between mature infectious individuals and immature susceptible individuals would only result in a slight increase in new infections. In particular, a 60% increase in parameter β_{ac2} could only lead to a 5.59% and 4.28% increase in the peak size and cumulative number of infections in 2017–2018, respectively. It follows from Figs. 6c and 7c that increasing the isolation rate of immature infectious individuals would lead to a significant decline in new infections, whereas Figs. 6d and 7d indicate that decreasing the incubation period $(1/\sigma_c)$ would result in a slight increase in new infections. The main results demonstrate that the transmission between immature individuals has a significant impact on the spread of HFMD, whereas transmission between mature infectious and immature susceptible individuals has a weak effect on the spread of the disease. Transmission between immature individuals thus plays a key role in the HFMD spread. All these factors have a more significant effect on the peak size than on the cumulative size.

To further investigate the impact of some key factors on HFMD outbreaks, we analyzed the sensitivity of the average monthly number of the immature infectious individuals with respect to the corresponding parameters. We computed the partial

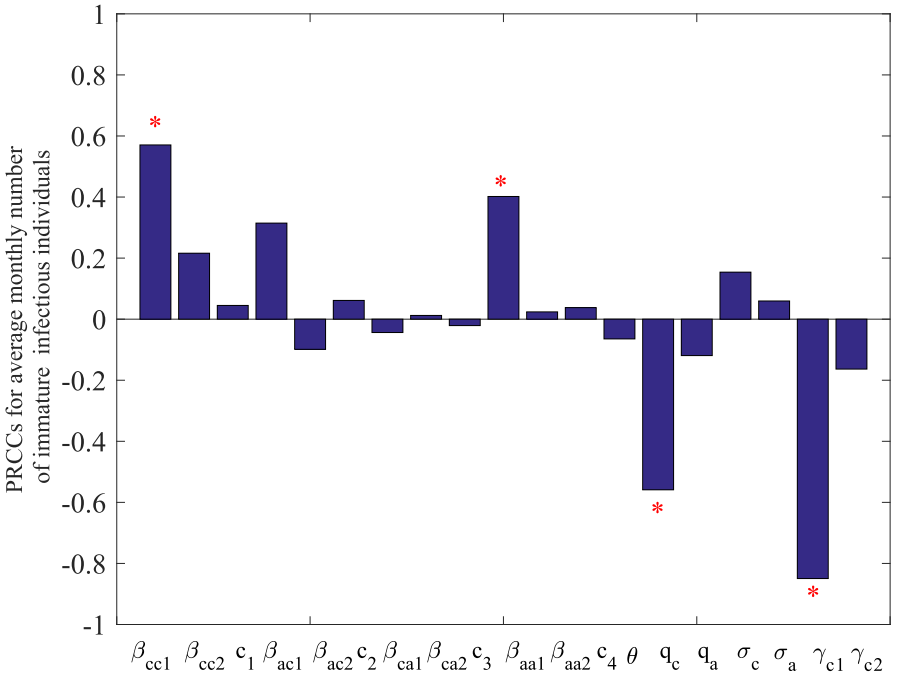

Fig. 8 Partial rank correlation coefficients (PRCCs) of the average monthly number of immature infectious individuals. The four significant parameters are noted

rank correlation coefficients (PRCCs) using Latin Hypercube Sampling (LHS). By computing the rank-transformed LHS matrix and the output matrix, we calculated PRCCs, which allows us to assess whether one parameter has significant effect on the average monthly number of the immature infectious individuals. LHS was performed with 5,000 bins and 2920 simulations per sampling, as shown in Fig. 8. We considered absolute values of PRCCs greater than 0.4 as indicating significant correlations between the parameters and the average monthly number of immature infectious individuals, values between 0.2 and 0.4 as moderate correlations, and values less than 0.2 as not significant. In the first half of Sect. 4.2, we show that the number of new infections of HFMD is related to the infection rate between immature individuals $\beta_{cc}(t)$ or between immature susceptible individuals and mature infected individuals $\beta_{ac}(t)$. In fact, these two transmission-rate functions contain many parameters, so which specific parameter has a greater impact on the transmission of HFMD is still unclear. Therefore, we have analyzed each parameter of the infection rate function here. Figure 8 indicates that most significant parameters are β_{cc1}, the transmission rate between immature infectious individuals and immature susceptibles; β_{aa1}, the transmission rate between mature infectious individuals and mature susceptibles; q_c, the isolation rate of immature infectious individuals; and γ_{c1}, the recovery rate of immature infectious individuals.

In order to reveal how the periodic transmission and the control measures affect the outbreak risk of HFMD in mainland China, we qualitatively assessed the exact impact

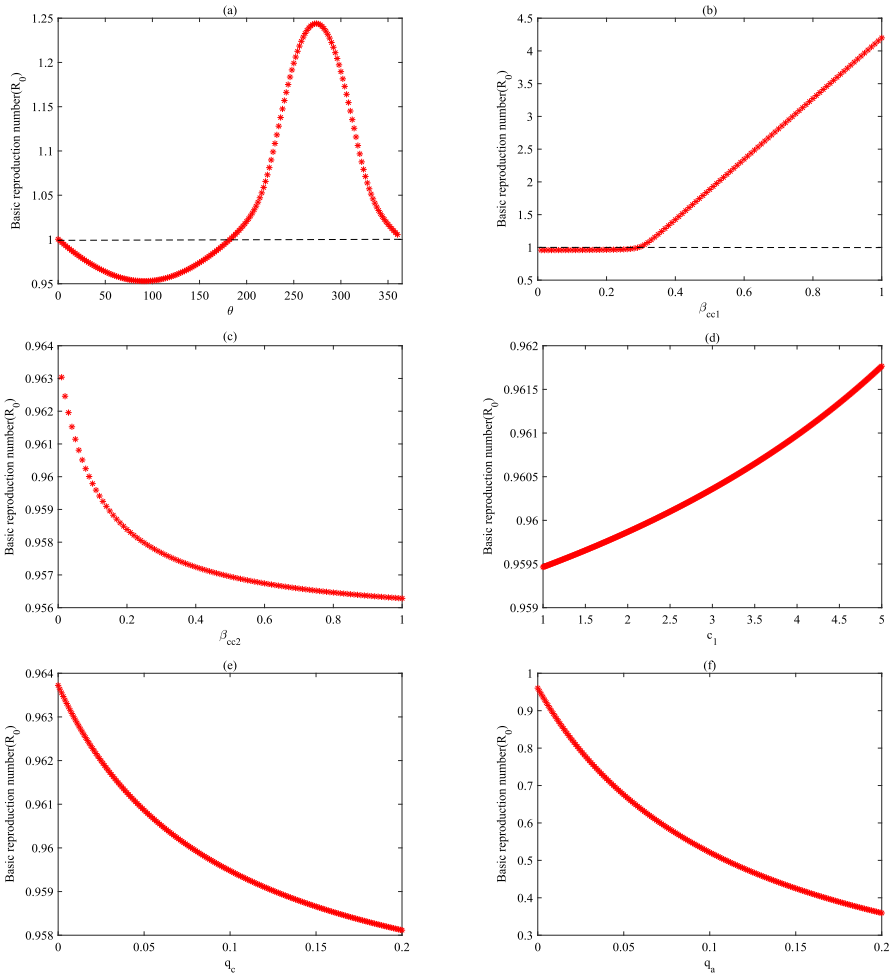

Fig. 9 Sensitivity analysis of R_0 with respect to the parameters θ, β_{cc1}, β_{cc2}, c_1, q_c and q_a. The dashed grey lines indicate $R_0 = 1$, and the red asterisks show the changes in the basic reproduction number R_0 as the parameters vary

of the transmission rate between the immature infectious individuals and susceptibles (i.e., β_{cc}) and the isolation rates (i.e., q_c, q_a) on the basic reproduction number. We plotted the variation of R_0 as the parameters related to β_{cc} (i.e., θ, β_{cc1}, β_{cc2} and c_1) and let the isolation rates vary, as shown in Fig. 9. In Fig. 9, the red asterisk points indicate how the basic reproduction number R_0 varies with the discontinuous variation in the parameters. However, in other figures—for example, Fig. 5—the basic reproduction number R_0 varies continuously with respect to time, so we adopted lines in our plotting. Fig. 9a shows that R_0 would decrease if parameter θ was increased from 0° to 90° or from 275° to 360°, whereas R_0 would increase if θ was increased from 90 to 275. Significantly, θ can make the reproduction number R_0 higher than 1 when it increases beyond 185°. It follows from Fig. 9b that the R_0 would increase as β_{cc1} increases.

If β_{cc1} exceeded 0.3, R_0 would increase almost linearly, so a small increase in β_{cc1} could lead to a large increase in R_0. When $\beta_{cc1} > 0.3$, $R_0 > 1$. From Fig. 9c, a decline would occur in R_0 if β_{cc2} was increased, although it would only trigger a small decrease in R_0. Figure 9d indicates that even substantial increase in c_1 would only trigger a small increase in R_0. According to Fig. 9e and f, if the isolation rates q_c and q_a were increased, R_0 would decrease. Varying q_a would trigger more change in the basic reproduction number R_0 if the same variation occurs for q_c as q_a. The main findings indicate that those parameters related to the transmission rate and the isolation rates have a significant effect on the basic reproduction number R_0. Reducing the social activities as well as enhancing isolation measures could reduce the outbreak risk of HFMD significantly. In particular, the outbreak can be controlled if q_a is large enough (i.e., if enough mature individuals can be isolated).

It is worth noting that Fig. 8 demonstrates that enhancing the isolation of immature infectious individuals (q_c) would result in a significant decrease in the average monthly number of immature infectious individuals in a cycle, but enhancing the isolation of mature infectious individuals (q_a) would only have a somewhat small effect on the average monthly number of immature infections. That is reasonable, since we focus on the immature infections here. However, Fig. 9 indicates that strengthening isolation of the mature infectious individuals (q_a) would lead to a significant decrease in the outbreak risk, whereas strengthening the isolation of immature infectious individuals would affect the outbreak risk only marginally. This suggests that a factor that has a significant impact on outbreak risk does not necessarily have a significant impact on the cumulative number of infections in a cycle. This may be because the cumulative number of infections in a cycle is affected by other factors besides the basic reproduction number.

5 Optimal control

In this section, we aim to apply controls in the targeted model to examine potential outcomes using optimal-control theory. Optimal-control theory for models with underlying dynamics governed by a system of ordinary differential equations was formulated by Pontryagin and Boltyanskii. According to Pontryagin's Maximum Principle (Pontryagin et al. 1962), we can investigate the necessary conditions of an optimal control if the optimal control exists. We then proceed by numerically solving the optimal control system to obtain the desired optimal control. We consider two different objective functionals to control and stop the spread of HFMD in the following. In the first scenario, we consider the disease burden as well as the cost required to curb the disease in the objective functional. For simplicity, we will refer to the optimal-control model with this objective functional as the disease burden with cost (DBC). In the second, the objective functional is a combination of new infections and the cost; for simplicity, we will refer to the optimal-control model with this objective functional as new infections with cost (NIC).

5.1 Disease burden with cost (DBC)

In order to demonstrate our idea, we first consider a simple case. Since the immature population is the main infected population of HFMD in mainland China, we first investigate optimal-control measures to curb the spread of HFMD in mainland China by strengthening containments to reduce infection in the immature population. Based on the results of sensitivity analysis, we initially choose the transmission rates $\beta_{cc}(t)$ and $\beta_{ac}(t)$ as control parameters and design the following optimal-control strategy: reducing the transmission rate $\beta_{cc}(t)$ and $\beta_{ac}(t)$ by $u_1(t)$ and $u_2(t)$, respectively, where $1-u_1(t)$ and $1-u_2(t)$ measure precautionary efforts such as media reporting, hand washing and social distancing. The model incorporating these controls is governed by the following differential equations:

$$\begin{aligned}
\frac{dS_c(t)}{dt} &= \Lambda - \frac{\beta_{cc}(t)(1-u_1(t))S_cI_c}{N_c} - \frac{\beta_{ac}(t)(1-u_2(t))S_cI_a}{N_c} - \mu S_c - \phi S_c + \rho_c R_c,\\
\frac{dE_c(t)}{dt} &= \frac{\beta_{cc}(t)(1-u_1(t))S_cI_c}{N_c} + \frac{\beta_{ac}(t)(1-u_2(t))S_cI_a}{N_c} - \mu E_c - \sigma_c E_c,\\
\frac{dI_c(t)}{dt} &= \sigma_c E_c - q_c I_c - \gamma_{c_1} I_c - \mu I_c - \alpha_{c_1} I_c,\\
\frac{dQ_c(t)}{dt} &= q_c I_c - \gamma_{c_2} Q_c - \mu Q_c - \alpha_{c_2} Q_c,\\
\frac{dR_c(t)}{dt} &= \gamma_{c_1} I_c + \gamma_{c_2} Q_c - \mu R_c - \phi R_c - \rho_c R_c,\\
\frac{dS_a(t)}{dt} &= \phi S_c - \mu S_a + \rho_a R_a - \frac{\beta_{ca}(t)S_aI_c}{N_a} - \frac{\beta_{aa}(t)S_aI_a}{N_a},\\
\frac{dE_a(t)}{dt} &= \frac{\beta_{ca}(t)S_aI_c}{N_a} + \frac{\beta_{aa}(t)S_aI_a}{N_a} - \mu E_a - \sigma_a E_a,\\
\frac{dI_a(t)}{dt} &= \sigma_a E_a - q_a I_a - \gamma_{a_1} I_a - \mu I_a - \alpha_{a_1} I_a,\\
\frac{dQ_a(t)}{dt} &= q_a I_a - \gamma_{a_2} Q_a - \mu Q_a - \alpha_{a_2} Q_a,\\
\frac{dR_a(t)}{dt} &= \phi R_c + \gamma_{a_1} I_a + \gamma_{a_2} Q_a - \mu R_a - \rho_a R_a.
\end{aligned} \tag{16}$$

The aim is to find the optimal values u_1^* and u_2^* of the controls u_1 and u_2 such that the associated trajectories $S_c(t)$, $E_c(t)$, $I_c(t)$, $Q_c(t)$, $R_c(t)$, $S_a(t)$, $E_a(t)$, $I_a(t)$, $Q_a(t)$ and $R_a(t)$ solve system (16) in the time interval $[0, t_{end}]$ with initial conditions $S_c(0)$, $E_c(0)$, $I_c(0)$, $Q_c(0)$, $R_c(0)$, $S_a(0)$, $E_a(0)$, $I_a(0)$, $Q_a(0)$ and $R_a(0)$ while minimizing the objective functional. The objective functional is defined as the sum of the cumulative costs associated with the disease $J_{n1}(u_1, u_2)$ and the cost of intervention $J_{c1}(u_1, u_2)$; i.e.,

$$\min_{u_i(t)\in U_1} \{J_{n1}(u_1, u_2) + J_{c1}(u_1, u_2)\} \tag{17}$$

where $U_1 = \{(u_1, u_2) \in L^1[0, t_{end})] | 0 \leq u_i \leq u_{i_{max}}, i = 1, 2\}$ and $J_{n1}(u_1, u_2)$ and $J_{c1}(u_1, u_2)$ are functions of control efforts $u_i(t)$, $i = 1, 2$. The control variables are assumed to be Lebesgue measurable on a finite interval $[0, t_{end}]$. The cost related to the disease depends on the available information and specific disease-containment measures, which can be expressed as

$$J_{n1}(u_1, u_2) = \int_0^{t_{end}} [A_1 I_c(t) + A_2 I_a(t)] dt,$$

where A_1 and A_2 are positive scaling coefficients used to represent the mean monetary value of each day of illness (i.e., loss of productivity and drug treatment) and the value of lives lost. $J_{n1}(u_1, u_2)$ represents the total cost of treatment, loss of productivity and lives lost of current infecteds per day during spread of HFMD. The total cost of intervention is a nonlinear function of $u_i(t)$,

$$J_{c1}(u_1, u_2) = \int_0^{t_{end}} \left[B_1 u_1^2(t) + B_2 u_2^2(t)\right] dt,$$

where B_1 and B_2 are positive constants accounting for the cost of intervention. We choose a nonlinear function for the intervention cost to ensure the existence of optimal control.

Theorem 3 *For system (16), there exists adjoint functions $\lambda_i (i = 1, 2, \cdots, 10)$ and optimal controls u_1^* and u_2^* that minimize the objective functional (17) on U_1, where*

$$\begin{aligned} u_1^* &= \min\left\{u_{1_{max}}, \max\left\{0, \frac{(\lambda_2 - \lambda_1)\beta_{cc}(t) S_c I_c}{2 N_c B_1}\right\}\right\}, \\ u_2^* &= \min\left\{u_{2_{max}}, \max\left\{0, \frac{(\lambda_2 - \lambda_1)\beta_{ac}(t) S_c I_a}{2 N_c B_2}\right\}\right\}, \end{aligned} \tag{18}$$

$\lambda_i' = -\frac{\partial H_1}{\partial z_i}$ *with the transversality conditions* $\lambda_i(t_{end}) = 0 (i = 1, \cdots, 10)$ *and* $(z_1, z_2, z_3, z_4, z_5, z_6, z_7, z_8, z_9, z_{10})^T = (S_c, E_c, I_c, Q_c, R_c, S_a, E_a, I_a, Q_a, R_a)^T$.

For the detailed derivation of the adjoint functions λ_i and optimal controls (18), see Appendix B. For the proof of Theorem 3, see Appendix D.

5.2 New infections with cost (NIC)

In this section, we focus on the optimal-control strategy to contain the transmission of HFMD in mainland China by decreasing the infections and isolating more infecteds. We choose the transmission rates $\beta_{cc}(t)$, $\beta_{ac}(t)$, $\beta_{ca}(t)$, $\beta_{aa}(t)$ and isolation rates q_c, q_a as control parameters and design the following optimal-control strategy: reducing the above transmission rates by $u_1(t)$, $u_2(t)$, $u_3(t)$ and $u_4(t)$, respectively, and improving the isolation rates q_c and q_a by $u_5(t)$ and $u_6(t)$, respectively, where $1 - u_1(t)$, $1 - u_2(t)$, $1 - u_3(t)$ and $1 - u_4(t)$ measure precautionary efforts such as

media reporting, hand-washing and social distancing, while $1 + u_5(t)$ and $1 + u_6(t)$ measure viral-load detection. The monetary cost of disease can be estimated as a flat rate associated to each infected case and derived from the total number of infected cases (Igoe et al. 2023).

In the second scenario, we do not consider the deaths but only consider the number of new infections. Hence we adopt a different objective functional that considers the number of new infecteds instead of current infecteds. Similarly, the control parameters are functions of time appearing as coefficients in the model. The control efforts $u_i(t)$, $i = 1, 2, \ldots, 6$, are assumed to be subject to constraints $0 \leq u_i(t) \leq u_{i_{max}}$, $i = 1, \ldots, 6$, $t \in [0, t_{end}]$. The model incorporating the six control variables is given by the following equations:

$$\begin{aligned}
\frac{dS_c(t)}{dt} &= \Lambda - \frac{\beta_{cc}(t)(1-u_1(t))S_cI_c}{N_c} - \frac{\beta_{ac}(t)(1-u_2(t))S_cI_a}{N_c} - \mu S_c - \phi S_c + \rho_c R_c,\\
\frac{dE_c(t)}{dt} &= \frac{\beta_{cc}(t)(1-u_1(t))S_cI_c}{N_c} + \frac{\beta_{ac}(t)(1-u_2(t))S_cI_a}{N_c} - \mu E_c - \sigma_c E_c,\\
\frac{dI_c(t)}{dt} &= \sigma_c E_c - q_c(1+u_5(t))I_c - \gamma_{c_1} I_c - \mu I_c - \alpha_{c_1} I_c,\\
\frac{dQ_c(t)}{dt} &= q_c(1+u_5(t))I_c - \gamma_{c_2} Q_c - \mu Q_c - \alpha_{c_2} Q_c,\\
\frac{dR_c(t)}{dt} &= \gamma_{c_1} I_c + \gamma_{c_2} Q_c - \mu R_c - \phi R_c - \rho_c R_c,\\
\frac{dS_a(t)}{dt} &= \phi S_c - \mu S_a + \rho_a R_a - \frac{\beta_{ca}(t)(1-u_3(t))S_aI_c}{N_a} - \frac{\beta_{aa}(t)(1-u_4(t))S_aI_a}{N_a},\\
\frac{dE_a(t)}{dt} &= \frac{\beta_{ca}(t)(1-u_3(t))S_aI_c}{N_a} + \frac{\beta_{aa}(t)(1-u_4(t))S_aI_a}{N_a} - \mu E_a - \sigma_a E_a,\\
\frac{dI_a(t)}{dt} &= \sigma_a E_a - q_a(1+u_6(t))I_a - \gamma_{a_1} I_a - \mu I_a - \alpha_{a_1} I_a,\\
\frac{dQ_a(t)}{dt} &= q_a(1+u_6(t))I_a - \gamma_{a_2} Q_a - \mu Q_a - \alpha_{a_2} Q_a,\\
\frac{dR_a(t)}{dt} &= \phi R_c + \gamma_{a_1} I_a + \gamma_{a_2} Q_a - \mu R_a - \rho_a R_a.
\end{aligned} \tag{19}$$

We assume that the transmission rates $\beta_{cc}(t)$, $\beta_{ac}(t)$, $\beta_{ca}(t)$ and $\beta_{aa}(t)$ are reduced by $u_1(t)$, $u_2(t)$, $u_3(t)$ and $u_4(t)$, respectively, and that the isolation rates q_c and q_a are increased by $u_5(t)$ and $u_6(t)$, respectively. The combined objective functional takes the form

$$\min_{u_i(t) \in U_2} \{J_{n2}(u_1, \cdots, u_6) + J_{c2}(u_1, \cdots, u_6)\}, \tag{20}$$

where $U_2 = \{(u_1, u_2, u_3, u_4, u_5, u_6) \in L^1[0, t_{end}] | 0 \leq u_i \leq u_{i_{max}}, i = 1, 2, ..., 6\}$ and

$$
\begin{aligned}
J_{c2}(u_1(t),\cdots,u_6(t)) &= \int_0^{t_{end}} \left[B_1u_1^2(t)+B_2u_2^2(t)\right.\\
&\quad \left.+B_3u_3^2(t)+B_4u_4^2(t)+B_5u_5^2(t)+B_6u_6^2(t)\right]dt,\\
J_{n2}(u_1(t),\cdots,u_6(t)) &= \int_0^{t_{end}} \left[A_1\left(\frac{\beta_{cc}(t)(1-u_1(t))S_cI_c}{N_c}+\frac{\beta_{ac}(t)(1-u_2(t))S_cI_a}{N_c}\right)\right.\\
&\quad \left.+A_2\left(\frac{\beta_{ca}(t)(1-u_3(t))S_aI_c}{N_a}+\frac{\beta_{aa}(t)(1-u_4(t))S_aI_a}{N_a}\right)\right]dt.
\end{aligned}
$$

Here $B_1, B_2, B_3, B_4, B_5, B_6, A_1$ and A_2 are positive constants. The specific form of the optimal control is affected by the relative values of the coefficients A_1, A_2, B_1, B_2, B_3, B_4, B_5 and B_6. We similarly get the following conclusion.

Theorem 4 *For system (19), there exist adjoint functions $\lambda_i (i = 1, 2, \cdots, 10)$ and optimal controls $u_1^*, u_2^*, u_3^*, u_4^*, u_5^*, u_6^*$ that minimize the objective functional (20) on U_2, where the optimal controls $u_i^* (i = 1, 2, \cdots, 6)$ are given by*

$$
\begin{aligned}
u_1^* &= \min\left\{u_{1_{\max}}, \max\left\{0, \frac{(\lambda_2+A_1-\lambda_1)\beta_{cc}(t)S_cI_c}{2N_cB_1}\right\}\right\},\\
u_2^* &= \min\left\{u_{2_{\max}}, \max\left\{0, \frac{(\lambda_2+A_1-\lambda_1)\beta_{ac}(t)S_cI_a}{2N_cB_2}\right\}\right\},\\
u_3^* &= \min\left\{u_{3_{\max}}, \max\left\{0, \frac{(\lambda_7+A_2-\lambda_6)\beta_{ca}(t)S_aI_c}{2N_aB_3}\right\}\right\},\\
u_4^* &= \min\left\{u_{4_{\max}}, \max\left\{0, \frac{(\lambda_7+A_2-\lambda_6)\beta_{aa}(t)S_aI_a}{2N_aB_4}\right\}\right\},\\
u_5^* &= \min\left\{u_{5_{\max}}, \max\left\{0, \frac{(\lambda_3-\lambda_4)q_cI_c}{2B_5}\right\}\right\},\\
u_6^* &= \min\left\{u_{6_{\max}}, \max\left\{0, \frac{(\lambda_8-\lambda_9)q_aI_a}{2B_6}\right\}\right\},
\end{aligned}
\tag{21}
$$

$\lambda_i' = -\frac{\partial H_2}{\partial z_i}$ with the transversality conditions $\lambda_i(t_{end}) = 0 (i = 1, \cdots, 10)$ and $(z_1, z_2, z_3, z_4, z_5, z_6, z_7, z_8, z_9, z_{10})^T = (S_c, E_c, I_c, Q_c, R_c, S_a, E_a, I_a, Q_a, R_a)^T$.

For detailed derivation of the optimal control, see Appendix C.

5.3 Simulations of optimal systems

We discuss the numerical solutions of the optimal systems and the corresponding control measures in the following. We use the approximate algorithm to obtain the optimal control based on the forward–backward sweep scheme with a first-order Runge–Kutta scheme that is proposed in Pontryagin (1985), Lenhart and Workman (2007). We use a convex combination to speed up the convergence, and the specific process is as follows. Update u_i by substituting the new adjoint variables λ_i, $(i = 1, \ldots, 10)$ into

(18) and (21). They are not stored as the control u_i, but as temporary vectors $\overline{u}_i$. The control variables u_i are set as the convex combination of the values of the last iteration of u_i, namely, $oldu_i$, and the temporary vectors $\overline{u}_i$. That is,

$$u_i = c\overline{u}_i + (1-c)oldu_i,$$

where $c \in (0, 1)$. Here, we choose $c = 0.5$. Once the values of the control variables u_i at the present iteration are sufficiently close to those at the previous iteration, the iteration is suspended. We initially solve the optimal model under the DBC strategy using the parameters reported in Tables 1 and 2. We assume the controls $u_1(t)$ and $u_2(t)$ in the optimal control model (16) and the objective functional (17) are constant controls, and we can derive the optimal controls $u_1 = 0.1320$ and $u_2 = 0.0535$, which minimize the objective functional (17). Hence, in Table 2, we adopt $u_1 = 0.1320$, $u_2 = 0.0535$ in the constant-control case. We tested the advantage of optimal control as compared to constant control using data on the immature HFMD cases in 2018, as shown in Table 2 and Fig. 10. In Table 2, we adopt CombOC and ConstC to denote combined optimal control and constant control. In Table 2, diff (I) and diff (II) refer to the difference between the optimal control and either the no-control case or constant control, respectively. In Fig. 10, the red, green and blue curves represent the effects of no control, constant control and optimal control on the transmission rate and the cumulative number of immature HFMD cases, respectively. Subplots (a) and (b) illustrate the variation of the transmission rate $\beta_{cc}(t)$ and the cumulative number of immature HFMD cases under different controls, respectively. It follows from Table 2 and Fig. 10 that the cumulative number of immature HFMD cases is much smaller in the case of optimal control (9.5023×10^5 cases) than the case of no control (1.69706×10^6 cases) or constant control (9.9091×10^5 cases), with a reduction of 44% and 4.11%, respectively. Optimal control results in a lower total cost than the cost in the case with constant control (8.28% lower) or no-control case (31% lower) and leads to a lower number of deaths (37) than the deaths in the case with constant control (38 deaths) or the case without control (66 deaths), with a reduction of 2.63% and 44%, respectively. Figure 10c–d demonstrate that the optimal controls $u_1(t)$ and $u_2(t)$ are time varying, staying at the maximum for approximately 2 months and 4 months, respectively, and then decreasing. From Table 2 and Fig. 10, we can intuitively see that optimal control has the best effect, which minimizes total cost, the number of infections and the sum of deaths.

Note that it is difficult to obtain the estimates of the cost of controls in particular for nonlinear cost parameters (i.e., the values of B_1 and B_2), so we fix A_1 and A_2 and vary the magnitude of B_1 and B_2 to examine the advantage of optimal control. Varying the magnitude of the non-linear control parameters led to a similar result: optimal control has advantages besides minimizing total cost, such as saving lives and reducing infections (Appendix F, Fig. 14, Table 5).

Next, we use the parameters reported in Tables 1 and 3 to solve the optimal model under the NIC strategy. Given that there are six controls in the NIC strategy, the maximum value for each control need not be as large as the corresponding value in the DBC strategy but can be slightly smaller than the value in the DBC strategy. Thus, in this scenario, we assume the bounds of the six optimal controls are $u_{1max} = 0.06$,

Table 2 Results of the DBC strategy with time horizon of 365 days in 2018 and difference between optimal control and constant control or no-control case, using $A_1 = 1$, $A_2 = 1$, $B_1 = 150000$, $B_2 = 130000$, $u_{1max} = 0.15$ and $u_{2max} = 0.1$

	No control	CombOC	ConstC	diff(I) (%)	diff(II) (%)
Cumulative immature HFMD cases	1.69706×10^6	9.5023×10^5	9.9091×10^5	−44	−4.11
Disease cost $J_{n1}(u_1, u_2)$	9.072×10^6	5.5579×10^6	5.7407×10^6	−43	−3.18
Intervention cost $J_{c1}(u_1, u_2)$	0	7.0433×10^5	1.0868×10^6	–	−35.19
Total cost	9.072×10^6	6.2622×10^6	6.8275×10^6	−31	−8.28
Total deaths	66	37	38	−44	−2.63
Max number of infected	6.1209×10^4	2.7237×10^4	3.0025×10^4	−56	−9.29

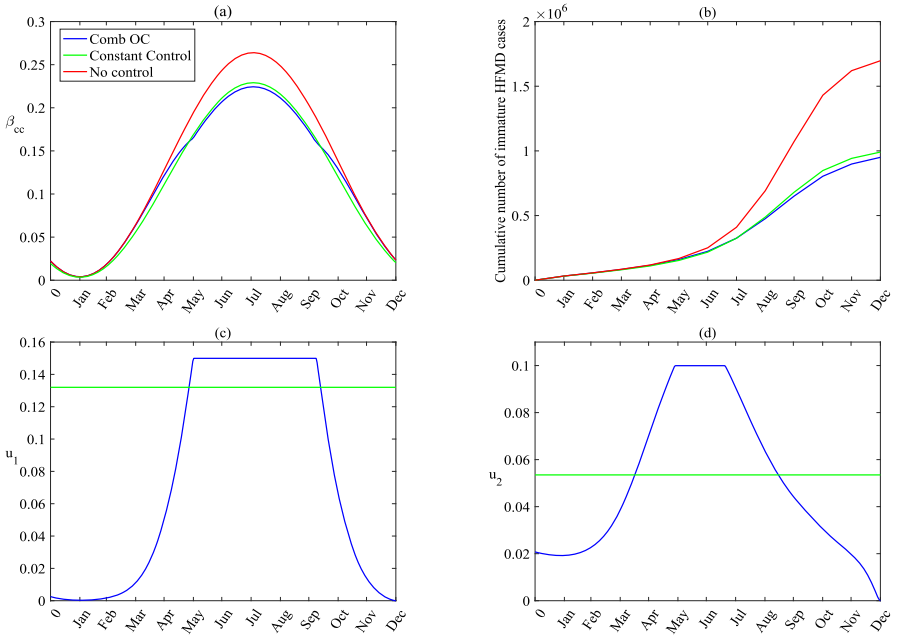

Fig. 10 Optimal control and cumulative number of immature HFMD cases for the DBC strategy compared to a constant control and the no-control cases, with parameters as in Tables 1 and 2. **a** Comparison of the transmission rate $\beta_1(t)$ with the combined optimal control (blue), constant control (green) and no control (red). **b** Comparison of the cumulative number of immature HFMD cases in 2018 with the combined optimal control (blue), constant control (green) and no control (red). **c**–**d** Optimal controls $u_1(t)$ and $u_2(t)$

$u_{2max} = 0.017$, $u_{3max} = 0.002$, $u_{4max} = 0.02$, $u_{5max} = 0.02$ and $u_{6max} = 0.0002$. Performing a similar simulation to the first scenario (DBC), we derive the optimal controls $u_1 = 0.0420$, $u_2 = 0.0136$, $u_3 = 0.0012$, $u_4 = 0.0200$, $u_5 = 0.0160$ and $u_6 = 0.00012$ that minimize the objective functional (20) in the constant-control case. We similarly demonstrate the advantages of time-varying control over constant control by applying the results to the data on the immature HFMD cases in 2018. The results are shown in Table 3 and Fig. 11, indicating that the cumulative number of immature HFMD cases, total cost, total deaths and maximum number of infections were all significantly reduced by using combined optimal control. Similarly, we draw a conclusion for the change of nonlinear control coefficients: that is, the optimal control has certain advantages compared to other controls (Appendix F, Fig. 15 and Table 7).

Note that the per-capita daily productivity loss and drug treatment play a key role in estimating monetary cost of the disease, which will ultimately affect the optimal-control policy. So in the following analysis, in order to seek optimal-control measures, we will explore to what extent the value of per-capita daily productivity loss and drug treatment affect the cumulative number of HFMD cases, deaths and total cost. We will examine what would happen if the scaling coefficients accounting for the drug treatment and loss of productivity vary. First, we simulate the optimal model with the DBC strategy under two alternative assumptions, in which the unit cost A_1 is assumed to be 5 or 1 and A_2 is assumed to be 5 or 1 in the appropriate monetary units to measure

Table 3 Results of the NIC strategy with time horizon of 365 days in 2018 and difference between optimal control and constant control or no-control case, using $A_1 = 1$, $A_2 = 1$, $B_1 = 150000$, $B_2 = 130000$, $B_3 = 100000$, $B_4 = 100000$, $B_5 = 150000$, $B_6 = 100000$, $u_{1max} = 0.06$, $u_{2max} = 0.017$, $u_{3max} = 0.002$, $u_{4max} = 0.02$, $u_{5max} = 0.02$, $u_{6max} = 0.0002$

	No control	CombOC	ConstC	diff(I) (%)	diff(II) (%)
Cumulative immature HFMD cases	1.69706×10^6	1.0957×10^6	1.1528×10^6	−35	−4.95
Disease cost $J_{n2}(u_1, \ldots, u_6)$	1.8466×10^6	1.2064×10^6	1.2624×10^6	−35	−4.44
Intervention cost $J_{c2}(u_1, \ldots, u_6)$	0	1.0527×10^5	1.3366×10^5	–	−21.24
Total cost	1.8466×10^6	1.3117×10^6	1.3960×10^6	−29	−6.04
Total deaths	66	43	45	−35	−4.44
Max number of infected	6.1207×10^4	3.478×10^4	3.8158×10^4	−43	−8.85

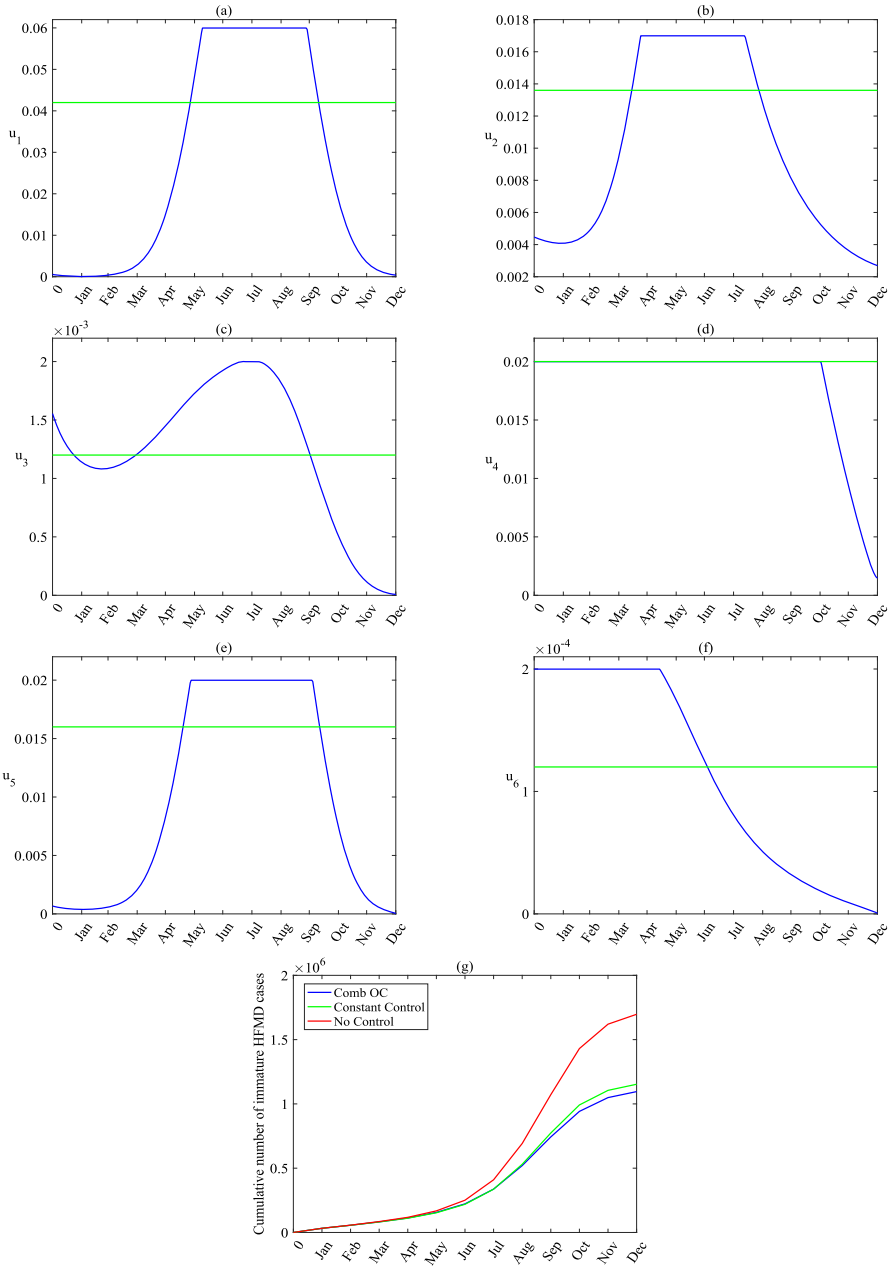

Fig. 11 Result of the NIC strategy compared to constant control and no control, with parameters as in Tables 1 and 3. **a–f** Optimal controls $u_1(t)$, $u_2(t)$, $u_3(t)$, $u_4(t)$, $u_5(t)$ and $u_6(t)$. **g** Comparison of the cumulative number of immature HFMD cases in 2018 with the combined optimal control (blue), constant control (green) and no control (red)

Table 4 Epidemiological values corresponding to Fig. 12 with the percentage differences measured from $A_1 = 5, A_2 = 5$ case

	$A_1 = 5, A_2 = 5$	$A_1 = 1, A_2 = 1$	% difference (%)
Cumulative immature HFMD cases	8.9692×10^5	9.5023×10^5	+5.94
Disease cost $J_{n1}(u_1, u_2)$	2.6543×10^7	5.5579×10^6	−79.06
Intervention cost $J_{c1}(u_1, u_2)$	1.1977×10^6	7.0433×10^5	−41.19
Total cost	2.7741×10^7	6.2622×10^6	−77.43
Total deaths	35	37	+5.71
Time spent at u_{1max}	205	130	−36.59
Time spent at u_{2max}	291	52	−82.13

The other control parameters are in Table 2

average productivity losses. The results are shown in Table 4 and Fig. 12. In Table 4 and Fig. 12, we use the same parameters as in Table 1 and the time horizon used in Table 2. It follows from Fig. 12 that the optimal control under different unit cost of the disease (i.e., A_1, A_2) affect the peak size, although they do not affect the peak time. If the unit cost of the disease is underestimated, simulations of the DBC strategy illustrate that the optimal strategy entails 5.94% more cases, 5.71% more lives lost, 77.43% less total cost and a 36.59% (resp., 82.13%) reduction in the number of days in which the transmission from the immature infectious individuals (mature infectious individuals) to immature susceptibles are at the maximum rate. We can derive a similar result for the NIC strategy, the details of which are presented in Appendix F. That demonstrates that the optimal-control measure would lead to more infections and more deaths, although it could result in less total cost if it was based on an underestimated per-capita cost of the disease. Therefore, a reasonable estimation of the per-capita value of the disease plays a critical role in determining the optimal-control strategy. It is worth emphasizing that the cost of control varies with the number of current infecteds or new infecteds, which demonstrates the importance of controlling the infection.

6 Discussion

To the best of our knowledge, our model is the first to incorporate a 2-year period in describing the outbreak of hand, foot and mouth disease in mainland China. We determined a threshold parameter $r(\Phi_{F-V}(\omega)) = 1$ that delineates extinction from uniform persistence in the form of a globally stable periodic orbit when $r(\Phi_{F-V}(\omega)) > 1$ (Theorem 2). By validating the model with data on the monthly number of HFMD cases among children under 7 in mainland China (Fig. 4), we estimated the basic reproduction number as 0.9599, which indicates that HFMD is unlikely to be eliminated if stochastic effects play a part. We also fitted the data with a periodic model of 1-year period (Fig. 13). By comparing the AIC values, we determined that a 2-year cycle was appropriate. We also analyzed the effective reproduction number over time and found that it fluctuated around 1 (Fig. 5).

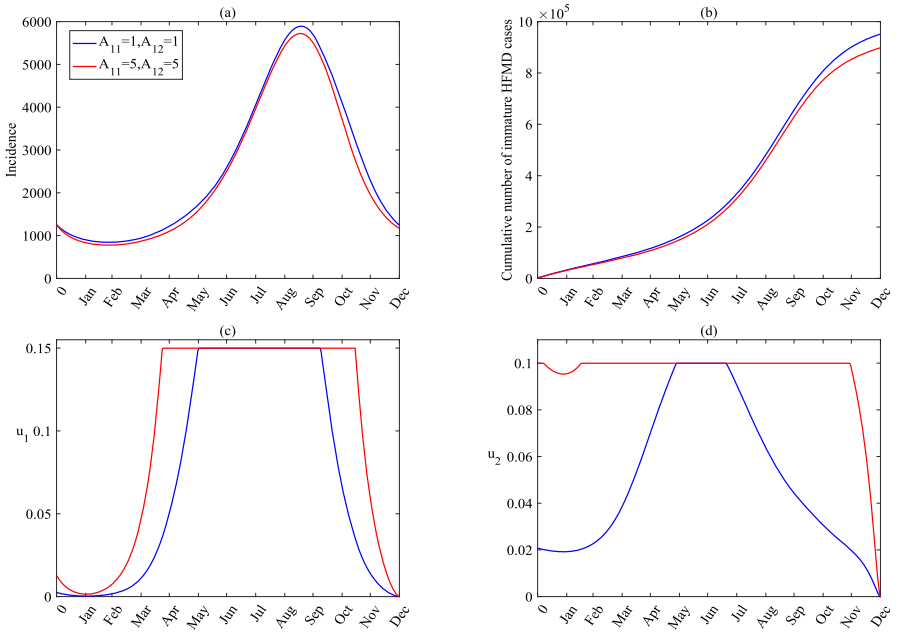

Fig. 12 Optimal control, incidence and cumulative number of immature HFMD cases in 2018 for the DBC strategy for different A_1, A_2 values corresponding to the results in Table 4

A sensitivity analysis implies that transmission between the immature/mature individuals (i.e., those under/above 7) is a critical factor. We also found that the epidemic could be controlled if sufficiently many mature infected individuals could be isolated (Figs. 6, 7, 8 and 9). We also applied two optimal-control schemes (DBC and NIC) to minimise the disease burden, new cases and overall costs of disease management, and the existence of optimal control was theoretically determined (Theorems 3 and 4). We showed that optimal control can have a substantial effect on lowering the cumulative cases compared to either no control or constant control (Table 2 and Fig. 10 for the DBC strategy; Table 3 and Fig. 11 for the NIC strategy). We also found that underestimating the per-capita cost of the disease would lead to more infections and more deaths, although it could result in less total cost (Fig. 12 and Table 4 for the DBC strategy; Fig. 16 and Table 9 for the NIC strategy. It follows that a reasonable estimation of the per-capita value of the disease is vital in determining the optimal-control strategy.

Our model has several limitations, which should be acknowledged. We used a double sinusoidal period, but the data is not perfectly sinusoidal. We only divided our population into two age groups: immature individuals under the age of 7 and mature individuals over the age of 7, whereas more subdivisions would yield more insights. A finer classification of the population would make the targeted model more realistic and reliable. For example, we could determine which age group has the most significant impact on the transmission of HFMD, and which age group of infected individuals can be isolated for better control in medical-resource constraints. However, the division of more stages would make the model higher-dimensional, resulting in more difficulties

in the fitting. We assumed a constant birth rate and a linear death rate, which are standard approximations in the field, but may not be the best formulations for large populations such as those found in mainland China. We have adopted six controls in the second optimal controls (i.e., the NIC strategy), but using fewer controls would be better. Future work could involve seeking the optimal strategy using fewer controls.

With such a low reproduction number, we stand a very real chance of eradicating hand and foot and mouth disease from mainland China. However, this will only happen if sufficient disease-control measures are undertaken. This requires mobilization of both individuals and governments, working in tandem to not only lower R_0 below the eradication threshold but keep it there.

Appendix A: Proof of Theorem 2

Proof We initially prove system (9) is uniformly persistent; i.e., there exists a constant $\varepsilon > 0$ such that the solution of system (9) with the arbitrary initial value

$$\left(S_c^0, E_c^0, I_c^0, Q_c^0, R_c^0, S_a^0, E_a^0, I_a^0, Q_a^0, R_a^0\right) \in \mathbb{R}_+^6 \times Int\left(\mathbb{R}_+^4\right)$$

satisfies

$$\begin{aligned}&\liminf_{t\to\infty}(S_c(t), E_c(t), I_c(t), Q_c(t), R_c(t), S_a(t), E_a(t), I_a(t), Q_a(t), R_a(t))\\ &\geq (\varepsilon, \varepsilon, \varepsilon, \varepsilon, \varepsilon, \varepsilon, \varepsilon, \varepsilon, \varepsilon, \varepsilon).\end{aligned}$$

Define P as the Poincaré map from $\mathbb{R}_+^{10} \to \mathbb{R}_+^{10}$ with $P(x_0) = u(\omega, x_0)$ for any $x_0 \in \mathbb{R}_+^{10}$, where $u(t, x_0)$ is the unique solution of system (9) satisfying $u(0, x_0) = x_0$. At first, we prove P is uniformly persistent with regard to $(X_0, \partial X_0)$. It follows from Lemmas 1 and 2 that X and X_0 are positively invariant and that ∂X_0 is a closed set in X. By Lemma 3, we know the solution of system (9) is uniformly and ultimately bounded, so P is point dissipative on $\mathbb{R}_+^{10}$. We further know that P is compact from $\mathbb{R}_+^{10}$ to $\mathbb{R}_+^{10}$. Therefore, P has a global attractor by Theorem 3.4.8 in Hale (2010). Define

$$\begin{aligned}M_\partial \equiv \Big\{&(S_c^0, E_c^0, I_c^0, Q_c^0, R_c^0, S_a^0, E_a^0, I_a^0, Q_a^0, R_a^0) \in \partial X_0\\ &: P^m(S_c^0, E_c^0, I_c^0, Q_c^0, R_c^0, S_a^0, E_a^0, I_a^0, Q_a^0, R_a^0) \in \partial X_0, m \geq 0\Big\}.\end{aligned}$$

Then we claim that

$$\begin{aligned}M_\partial = \big\{&(S_c, 0, 0, Q_c, R_c, S_a, 0, 0, Q_a, R_a) \in X : S_c \geq 0,\\ &Q_c \geq 0, R_c \geq 0, S_a \geq 0, Q_a \geq 0, R_a \geq 0\big\}.\end{aligned}$$

It is clear that

$$\big\{(S_c, 0, 0, Q_c, R_c, S_a, 0, 0, Q_a, R_a) \in X :$$

$$S_c \geq 0, Q_c \geq 0, R_c \geq 0, S_a \geq 0, Q_a \geq 0, R_a \geq 0\big\} \subseteq M_\partial.$$

And we just need to prove

$$M_\partial \subseteq \big\{(S_c, 0, 0, Q_c, R_c, S_a, 0, 0, Q_a, R_a) \in X : S_c \geq 0, Q_c \geq 0, R_c \geq 0, S_a \geq 0, Q_a \geq 0, R_a \geq 0\big\}.$$

For any

$$x_0 = \Big(S_c^0, E_c^0, I_c^0, Q_c^0, R_c^0, S_a^0, E_a^0, I_a^0, Q_a^0, R_a^0\Big) \in \partial X_0 \backslash \big\{(S_c, 0, 0, Q_c, R_c, S_a, 0, 0, Q_a, R_a) \in X : S_c \geq 0, Q_c \geq 0, R_c \geq 0, S_a \geq 0, Q_a \geq 0, R_a \geq 0\big\},$$

suppose any one of $\{E_c^0, I_c^0, E_a^0, I_a^0\}$ is not zero. Without loss of generality, let $E_c^0 = 0$, $I_c^0 = 0$, $E_a^0 > 0$, $I_a^0 = 0$. Then we obtain the following

$$\begin{aligned}
E_c(t) &= e^{-(\sigma_c+\mu)t}\int_0^t \Big(\frac{\beta_{cc}(u)S_cI_c}{N_c} + \frac{\beta_{ac}(u)S_cI_a}{N_c}\Big)e^{(\sigma_c+\mu)u}du > 0,\\
I_c(t) &= e^{-(q_c+\gamma_{c_1}+\alpha_{c_1}+\mu)t}\int_0^t \sigma_c E_c e^{(q_c+\gamma_{c_1}+\alpha_{c_1}+\mu)u}du > 0,\\
E_a(t) &= e^{-(\sigma_a+\mu)t}\left[E_a^0 + \int_0^t \Big(\frac{\beta_{ca}(u)S_aI_c}{N_a} + \frac{\beta_{aa}(u)S_aI_a}{N_a}\Big)e^{(\sigma_a+\mu)u}du\right] > 0,\\
I_a(t) &= e^{-(q_a+\gamma_{a_1}+\alpha_{a_1}+\mu)t}\int_0^t \sigma_a E_a e^{(q_a+\gamma_{a_1}+\alpha_{a_1}+\mu)u}du > 0
\end{aligned}$$

for any $t > 0$. Thus, we have

$$\big(S_c(t), E_c(t), I_c(t), Q_c(t), R_c(t), S_a(t), E_a(t), I_a(t), Q_a(t), R_a(t)\big) \notin \partial X_0,$$

so

$$M_\partial \subseteq \Big\{(S_c, 0, 0, Q_c, R_c, S_a, 0, 0, Q_a, R_a) : S_c \geq 0, Q_c \geq 0, R_c \geq 0, S_a \geq 0, Q_a \geq 0, R_a \geq 0\Big\}.$$

Therefore,

$$M_\partial = \Big\{(S_c, 0, 0, Q_c, R_c, S_a, 0, 0, Q_a, R_a) : S_c \geq 0, Q_c \geq 0, R_c \geq 0, S_a \geq 0, Q_a \geq 0, R_a \geq 0\Big\}.$$

It is clear that $E_0 = \left(\frac{\Lambda}{\phi+\mu}, 0, 0, 0, 0, \frac{\Lambda\phi}{\mu(\phi+\mu)}, 0, 0, 0, 0\right)$ is a fixed point of the map P in M_∂. Assume that

$$u(t, x_0) \equiv \big(S_c(t), E_c(t), I_c(t), Q_c(t), R_c(t), S_a(t), E_a(t), I_a(t), Q_a(t), R_a(t)\big)$$

is a solution of the system (9) satisfying $u(0, x_0) = x_0 \in M_\partial$, so we have

$$\frac{dQ_c}{dt} < 0, \frac{dR_c}{dt} < 0, \frac{dQ_a}{dt} < 0, \frac{dR_a}{dt} < 0$$

due to $E_c = 0, I_c = 0, E_a = 0, I_a = 0$. Thus we have

$$\lim_{t\to\infty} Q_c(t) = 0, \lim_{t\to\infty} R_c(t) = 0, \lim_{t\to\infty} Q_a(t) = 0, \lim_{t\to\infty} R_a(t) = 0,$$

so it follows that,

$$\lim_{t\to\infty} S_c(t) = \frac{\Lambda}{\mu+\phi}, \lim_{t\to\infty} S_a(t) = \frac{\Lambda\phi}{\mu(\mu+\phi)}.$$

We further have

$$\lim_{t\to\infty} \big(S_c(t), E_c(t), I_c(t), Q_c(t), R_c(t), S_a(t), E_a(t), I_a(t), Q_a(t), R_a(t)\big) = E_0,$$

so E_0 is isolated and $\{E_0\}$ is a cover without a cycle.

Next, we demonstrate $W^s(E_0) \cap X_0 = \emptyset$. For any $x_0 \in X_0$, by the continuity of solutions with respect to initial conditions, for any $\varepsilon > 0$, there exists $\delta_0 > 0$ such that when $\left|x_0 - E_0\right| \le \delta_0$, we have

$$\left\|u(t, x_0) - u(t, E_0)\right\| \le \varepsilon$$

for all $t \in [0, \omega]$. We claim that

$$\limsup_{m\to\infty} d\big(P^m(x_0), E_0\big) \ge \delta_0.$$

If not, then there exists $x^0 \in X_0$ such that

$$\limsup_{m\to\infty} d\big(P^m(x^0), E_0\big) < \delta_0. \tag{22}$$

Without loss of generality, we can assume that $d\big(P^m(x^0), E_0\big) < \delta_0$ holds for all $m > 0$, so

$$\left\|u(t, P^m(x^0)) - u(t, E_0)\right\| \le \varepsilon \text{ for all } t \in [0, \omega].$$

For any $t \geq 0$, let $t = m\omega + t_2$, where $t_2 \in [0, \omega)$ and $m = \left[\frac{t}{\omega}\right]$ is the greatest integer no larger than $\frac{t}{\omega}$. Thus

$$\left\| u(t, x^0) - u(t, E_0) \right\| = \left\| u(t_2, P^m(x^0)) - u(t_2, E_0) \right\| \leq \varepsilon$$

holds for all $t \geq 0$. Then we have

$$\begin{aligned}
&\frac{\Lambda}{\phi+\mu} - \varepsilon \leq S_c(t) \leq \frac{\Lambda}{\phi+\mu} + \varepsilon, \quad 0 \leq E_c(t) \leq \varepsilon, \quad 0 \leq I_c(t) \leq \varepsilon, \quad 0 \leq Q_c(t) \leq \varepsilon, 0 \leq R_c(t) \leq \varepsilon, \\
&\frac{\Lambda\phi}{\mu(\phi+\mu)} - \varepsilon \leq S_a(t) \leq \frac{\Lambda\phi}{\mu(\phi+\mu)} + \varepsilon, \quad 0 \leq E_a(t) \leq \varepsilon, \\
&\quad 0 \leq I_a(t) \leq \varepsilon, \quad 0 \leq Q_a(t) \leq \varepsilon, \quad 0 \leq R_a(t) \leq \varepsilon,
\end{aligned}$$

for all $t \geq 0$. Thus we get

$$\begin{aligned}
\frac{S_c(t)}{N_c(t)} &\geq \frac{\frac{\Lambda}{\phi+\mu} - \varepsilon}{\frac{\Lambda}{\phi+\mu} + 5\varepsilon} > \frac{\frac{\Lambda}{\phi+\mu} - \varepsilon - 5\varepsilon}{\frac{\Lambda}{\phi+\mu} + 5\varepsilon - 5\varepsilon} = \frac{\frac{\Lambda}{\phi+\mu} - 6\varepsilon}{\frac{\Lambda}{\phi+\mu}} = 1 - \frac{6\varepsilon}{\frac{\Lambda}{\phi+\mu}} \equiv 1 - \eta_1, \\
\frac{S_a(t)}{N_a(t)} &\geq \frac{\frac{\Lambda\phi}{\mu(\phi+\mu)} - \varepsilon}{\frac{\Lambda\phi}{\mu(\phi+\mu)} + 5\varepsilon} > \frac{\frac{\Lambda\phi}{\mu(\phi+\mu)} - \varepsilon - 5\varepsilon}{\frac{\Lambda\phi}{\mu(\phi+\mu)} + 5\varepsilon - 5\varepsilon} = \frac{\frac{\Lambda\phi}{\mu(\phi+\mu)} - 6\varepsilon}{\frac{\Lambda\phi}{\mu(\phi+\mu)}} = 1 - \frac{6\varepsilon}{\frac{\Lambda\phi}{\mu(\phi+\mu)}} \equiv 1 - \frac{\mu}{\phi}\eta_1,
\end{aligned}$$

where $\eta_1 = \frac{6\varepsilon}{\frac{\Lambda}{\phi+\mu}}$. Consider the auxiliary system

$$\begin{aligned}
\frac{dv_1}{dt} &= \beta_{cc}(t)(1-\eta_1)v_2 + \beta_{ac}(t)(1-\eta_1)v_4 - (\mu+\sigma_c)v_1, \\
\frac{dv_2}{dt} &= \sigma_c v_1 - (q_c + \gamma_{c_1} + \mu + \alpha_{c_1})v_2, \\
\frac{dv_3}{dt} &= \beta_{ca}(t)\big(1 - \eta_1\frac{\mu}{\phi}\big)v_2 + \beta_{aa}(t)\big(1 - \eta_1\frac{d}{\phi}\big)v_4 - (\mu+\sigma_a)v_3, \\
\frac{dv_4}{dt} &= \sigma_a v_3 - (q_a + \gamma_{a_1} + \mu + \alpha_{a_1})v_4.
\end{aligned}$$

Denote

$$D(t) = \begin{bmatrix}
-(\sigma_c+\mu) & \beta_{cc}(t)(1-\eta_1) & 0 & \beta_{ac}(t)(1-\eta_1) \\
\sigma_c & -(q_c+\gamma_{c_1}+\mu+\alpha_{c_1}) & 0 & 0 \\
0 & \beta_{ca}(t)\big(1-\eta_1\frac{\mu}{\phi}\big) & -(\sigma_a+\mu) & \beta_{aa}(t)\big(1-\eta_1\frac{\mu}{\phi}\big) \\
0 & 0 & \sigma_a & -(q_a+\gamma_{a_1}+\mu+\alpha_{a_1})
\end{bmatrix}.$$

It is easy to see that $D(t)$ is continuous, cooperative and irreducible. Let

$$F_1 = \begin{bmatrix} 0 & \beta_{cc}(t)(1-\eta_1) & 0 & \beta_{ac}(t)(1-\eta_1) \\ 0 & 0 & 0 & 0 \\ 0 & \beta_{ca}(t)(1-\eta_1\frac{\mu}{\phi}) & 0 & \beta_{aa}(t)(1-\eta_1\frac{\mu}{\phi}) \\ 0 & 0 & 0 & 0 \end{bmatrix},$$

$$V_1 = \begin{bmatrix} \sigma_c+\mu & 0 & 0 & 0 \\ -\sigma_c & q_c+\gamma_{c_1}+\mu+\alpha_{c_1} & 0 & 0 \\ 0 & 0 & \sigma_a+\mu & 0 \\ 0 & 0 & -\sigma_a & q_a+\gamma_{a_1}+\mu+\alpha_{a_1} \end{bmatrix},$$

Then we have

$$F_1 - V_1 = F - V - \eta_1 \begin{bmatrix} 0 & \beta_{cc}(t) & 0 & \beta_{ac}(t) \\ 0 & 0 & 0 & 0 \\ 0 & \beta_{ca}(t)\frac{\mu}{\phi} & 0 & \beta_{aa}(t)\frac{\mu}{\phi} \\ 0 & 0 & 0 & 0 \end{bmatrix} \equiv F - V - \eta_1 B(t).$$

By Lemma 5, we have $r\left(\Phi_{F-V}(\omega)\right) > 1$ if $R_0 > 1$. Thus when ε is sufficiently small, η_1 is small enough such that $r\left(\Phi_{F-V-\eta_1 B}(\omega)\right) > 1$. Hence, it follows from Lemma 3 and the comparison theorem that there exists a positive ω periodic function $v(t)$ such that $J(t) \geq v(t)e^{\theta_2 t}$ with

$$J(t) = \left(E_c(t), I_c(t), E_a(t), I_a(t)\right)^T, \theta_2 = \frac{1}{\omega}\ln\left(\Phi_{F-V-\eta_1 B}(t)\right).$$

Since $\theta_2 > 0$, we have

$$\lim_{t\to\infty} E_c(t) = \infty, \quad \lim_{t\to\infty} I_c(t) = \infty, \quad \lim_{t\to\infty} E_a(t) = \infty, \quad \lim_{t\to\infty} I_a(t) = \infty,$$

which contadicts (22). Thus $W^s(E_0) \cap X_0 = \emptyset$. So P is uniformly persistent, and further the solution of (9) is uniformly persistent. Thus, according to Theorem 1.3.6 in Zhao (2003), P has a fixed point

$$x_0^* \equiv \left(S_c^*(0), E_c^*(0), I_c^*(0), Q_c^*(0), R_c^*(0), S_a^*(0), E_a^*(0), I_a^*(0), Q_a^*(0), R_a^*(0)\right) \in X_0,$$

so

$$S_c^*(0) \in \mathbb{R}_+, \quad \left(E_c^*(0), I_c^*(0)\right) \in Int(\mathbb{R}_+^2), \quad \left(Q_c^*(0), R_c^*(0)\right) \in \mathbb{R}_+^2,$$
$$S_a^*(0) \in \mathbb{R}_+, \quad \left(E_a^*(0), I_a^*(0)\right) \in Int(\mathbb{R}_+^2), \quad \left(Q_a^*(0), R_a^*(0)\right) \in \mathbb{R}_+^2.$$

Suppose

$$S_c^*(0) > 0, Q_c^*(0) > 0, R_c^*(0) > 0, S_a^*(0) > 0, Q_a^*(0) > 0, R_a^*(0) > 0.$$

If not, we can let $S_c^*(0) = 0$, and it follows from the first equation of system (9) that

$$\frac{dS_c^*(t)}{dt} \geq \Lambda - \beta_{cc}(t)\frac{S_c^*(t)}{N_c}I_c - \beta_{ac}(t)\frac{S_c^*(t)}{N_c}I_a - (d+\phi)S_c^*(t)$$

and

$$S_c^*(0) = S_c^*(n\omega) = 0, n = 1, 2, 3, \ldots$$

Then we get

$$\begin{aligned} S_c^*(t) &\geq \left[S_c^*(0) + \int_0^t \Lambda e^{\int_0^{s_2}(\mu+\phi+\lambda_c(s_1))ds_1}ds_2\right]e^{\int_0^t -(\mu+\phi+\lambda_c(s_1))ds_1} \\ &= e^{\int_0^t -(\mu+\phi+\lambda_c(s_1))ds_1}\int_0^t \Lambda e^{\int_0^{s_2}(\mu+\phi+\lambda_c(s_1))ds_1}ds_2, \end{aligned}$$

so $S_c^*(n\omega) > 0$, which contradicts $S_c^*(n\omega) = 0$. It follows that $S_c^*(0) > 0$. Similarly, we can prove

$$Q_c^*(0) > 0, R_c^*(0) > 0, S_a^*(0) > 0, Q_a^*(0) > 0, R_a^*(0) > 0.$$

Therefore,

$$S_c^*(0) > 0, Q_c^*(0) > 0, R_c^*(0) > 0, S_a^*(0) > 0, Q_a^*(0) > 0, R_a^*(0) > 0$$

is a positive periodic solution with period ω. □

Appendix B: Optimal control of model (16)

The optimal control for the objective functional (17) can be found by Pontryagin's Maximum Principle (Pontryagin et al. 1962). In order to find the solution of the optimal system (16), we define the Hamiltonian function for the system as

$$\begin{aligned} H_1 = {} & A_1 I_c + A_2 I_a + B_1 u_1^2(t) + B_2 u_2^2(t) + \lambda_1\frac{dS_c}{dt} + \lambda_2\frac{dE_c}{dt} \\ & + \lambda_3\frac{dI_c}{dt} + \lambda_4\frac{dQ_c}{dt} + \lambda_5\frac{dR_c}{dt} \\ & + \lambda_6\frac{dS_a}{dt} + \lambda_7\frac{dE_a}{dt} + \lambda_8\frac{dI_a}{dt} + \lambda_9\frac{dQ_a}{dt} + \lambda_{10}\frac{dR_a}{dt} \end{aligned}$$

with the following adjoints and transversality conditions:

$$
\begin{aligned}
\lambda_1' = & -\Bigg[\lambda_6\phi + (\lambda_2-\lambda_1)\Bigg(\frac{\beta_{cc}(t)(1-u_1(t))I_c(N_c-S_c)}{N_c^2} \\
& + \frac{\beta_{ac}(t)(1-u_2(t))I_a(N_c-S_c)}{N_c^2}\Bigg) - \lambda_1(\mu+\phi)\Bigg] \\
\lambda_2' = & -\Bigg[(\lambda_1-\lambda_2)\Bigg(\frac{\beta_{cc}(t)(1-u_1(t))S_cI_c}{N_c^2} + \frac{\beta_{ac}(t)(1-u_2(t))S_cI_a}{N_c^2}\Bigg) \\
& - \lambda_2(\sigma_c+\mu) + \lambda_3\sigma_c\Bigg] \\
\lambda_3' = & -\Bigg[A_1 + (\lambda_2-\lambda_1)\Bigg(\frac{\beta_{cc}(t)(1-u_1(t))S_c(N_c-I_c)}{N_c^2} - \frac{\beta_{ac}(t)(1-u_2(t))S_cI_a}{N_c^2}\Bigg) \\
& - \lambda_3\big(q_c+\mu+\alpha_{c_1}+\gamma_{c_1}\big) + \lambda_4 q_c + \lambda_5\gamma_{c_1} + (\lambda_7-\lambda_6)\frac{\beta_{ca}(t)S_a}{N_a}\Bigg] \\
\lambda_4' = & -\Bigg[(\lambda_1-\lambda_2)\Bigg(\frac{\beta_{cc}(t)(1-u_1(t))S_cI_c}{N_c^2} + \frac{\beta_{ac}(t)(1-u_2(t))S_cI_a}{N_c^2}\Bigg) \\
& - \lambda_4\big(\mu+\alpha_{c_2}+\gamma_{c_2}\big) + \lambda_5\gamma_{c_2}\Bigg] \\
\lambda_5' = & -\Bigg[(\lambda_1-\lambda_2)\Bigg(\frac{\beta_{cc}(t)(1-u_1(t))S_cI_c}{N_c^2} + \frac{\beta_{ac}(t)(1-u_2(t))S_cI_a}{N_c^2}\Bigg) \\
& + \lambda_1\rho_c - \lambda_5(\mu+\phi+\rho_c) + \lambda_{10}\phi\Bigg] \\
\lambda_6' = & -\Bigg[(\lambda_7-\lambda_6)\Bigg(\frac{\beta_{ca}(t)I_c(N_a-S_a)}{N_a^2} + \frac{\beta_{aa}(t)I_a(N_a-S_a)}{N_a^2}\Bigg) - \lambda_6\mu\Bigg] \\
\lambda_7' = & -\Bigg[(\lambda_6-\lambda_7)\Bigg(\frac{\beta_{ca}(t)S_aI_c}{N_a^2} + \frac{\beta_{aa}(t)S_aI_a}{N_a^2}\Bigg) - \lambda_7(\sigma_a+\mu) + \lambda_8\sigma_a\Bigg] \\
\lambda_8' = & -\Bigg[A_2 + (\lambda_2-\lambda_1)\frac{\beta_{ac}(t)(1-u_2(t))S_c}{N_c} + (\lambda_6-\lambda_7)\Bigg(\frac{\beta_{ca}(t)S_aI_c}{N_a^2} - \frac{\beta_{aa}(t)S_a(N_a-I_a)}{N_a^2}\Bigg) \\
& - \lambda_8\big(q_a+\mu+\alpha_{a_1}+\gamma_{a_1}\big) + \lambda_9 q_a + \lambda_{10}\gamma_{a_1}\Bigg] \\
\lambda_9' = & -\Bigg[(\lambda_6-\lambda_7)\Bigg(\frac{\beta_{ca}(t)S_aI_c}{N_a^2} + \frac{\beta_{aa}(t)S_aI_a}{N_a^2}\Bigg) - \lambda_9\big(\mu+\alpha_{a_2}+\gamma_{a_2}\big) + \lambda_{10}\gamma_{a_2}\Bigg] \\
\lambda_{10}' = & -\Bigg[(\lambda_6-\lambda_7)\Bigg(\frac{\beta_{ca}(t)S_aI_c}{N_a^2} + \frac{\beta_{aa}(t)S_aI_a}{N_a^2}\Bigg) + \lambda_6\rho_a - \lambda_{10}(\mu+\rho_a)\Bigg]
\end{aligned}
$$

$\lambda_i(t_{end}) = 0, i = 1, \ldots, 10.$

On the interior of the control set, we can then characterize the optimal control by the optimality condition

$$
\begin{aligned}
\frac{\partial H_1}{\partial u_1}\bigg|_{u_1=u_1^*} &= 2B_1u_1 + \lambda_1\frac{\beta_{cc}(t)S_cI_c}{N_c} - \lambda_2\frac{\beta_{cc}(t)S_cI_c}{N_c} = 0, \\
\frac{\partial H_1}{\partial u_2}\bigg|_{u_2=u_2^*} &= 2B_2u_2 + \lambda_1\frac{\beta_{ac}(t)S_cI_a}{N_c} - \lambda_2\frac{\beta_{ac}(t)S_cI_a}{N_c} = 0.
\end{aligned}
$$

Then we have

$$u_1^* = \min\left\{u_{1_{max}}, \max\left\{0, \frac{(\lambda_2-\lambda_1)\beta_{cc}(t)S_cI_c}{2N_cB_1}\right\}\right\},$$
$$u_2^* = \min\left\{u_{2_{max}}, \max\left\{0, \frac{(\lambda_2-\lambda_1)\beta_{ac}(t)S_cI_a}{2N_cB_2}\right\}\right\}.$$

Appendix C: Optimal control of model (19)

The Hamiltonian function for model (19) is defined as:

$$\begin{aligned}H_2 = {} & A_1\left(\frac{\beta_{cc}(t)(1-u_1(t))S_cI_c}{N_c} + \frac{\beta_{ac}(t)(1-u_2(t))S_cI_a}{N_c}\right)\\ & + A_2\left(\frac{\beta_{ca}(t)(1-u_3(t))S_aI_c}{N_a} + \frac{\beta_{aa}(t)(1-u_4(t))S_aI_a}{N_a}\right)\\ & + B_1u_1^2(t) + B_2u_2^2(t) + B_3u_3^2(t) + B_4u_4^2(t) + B_5u_5^2(t) + B_6u_6^2(t)\\ & + \lambda_1\frac{dS_c}{dt} + \lambda_2\frac{dE_c}{dt} + \lambda_3\frac{dI_c}{dt} + \lambda_4\frac{dQ_c}{dt}\\ & + \lambda_5\frac{dR_c}{dt} + +\lambda_6\frac{dS_a}{dt} + \lambda_7\frac{dE_a}{dt} + \lambda_8\frac{dI_a}{dt} + \lambda_9\frac{dQ_a}{dt} + \lambda_{10}\frac{dR_a}{dt},\end{aligned}$$

where the adjoint variables satisfy the equations

$$\begin{aligned}\lambda_1' = {} & -\left[(\lambda_2 + A_1 - \lambda_1)\left(\frac{\beta_{cc}(t)(1-u_1(t))I_c(N_c-S_c)}{N_c^2}\right.\right.\\ & \left.\left. + \frac{\beta_{ac}(t)(1-u_2(t))I_a(N_c-S_c)}{N_c^2}\right) + \lambda_6\phi - \lambda_1(\mu+\phi)\right]\\ \lambda_2' = {} & -\left[(\lambda_1 - \lambda_2 - A_1)\left(\frac{\beta_{cc}(t)(1-u_1(t))S_cI_c}{N_c^2} + \frac{\beta_{ac}(t)(1-u_2(t))S_cI_a}{N_c^2}\right)\right.\\ & \left. - \lambda_2(\sigma_c+\mu) + \lambda_3\sigma_c\right]\\ \lambda_3' = {} & -\left[(\lambda_2 + A_1 - \lambda_1)\left(\frac{\beta_{cc}(t)(1-u_1(t))S_c(N_c-I_c)}{N_c^2} - \frac{\beta_{ac}(t)(1-u_2(t))S_cI_a}{N_c^2}\right)\right.\\ & - \lambda_3\left(q_c(1+u_5(t)) + \mu + \alpha_{c_1} + \gamma_{c_1}\right) + \lambda_4q_c(1+u_5(t)) + \lambda_5\gamma_{c_1}\\ & \left. + (\lambda_7 + A_2 - \lambda_6)\frac{\beta_{ca}(t)(1-u_3(t))S_a}{N_a}\right]\\ \lambda_4' = {} & -\left[(\lambda_1 - \lambda_2 - A_1)\left(\frac{\beta_{cc}(t)(1-u_1(t))S_cI_c}{N_c^2} + \frac{\beta_{ac}(t)(1-u_2(t))S_cI_a}{N_c^2}\right)\right.\\ & \left. - \lambda_4\left(\mu + \alpha_{c_2} + \gamma_{c_2}\right) + \lambda_5\gamma_{c_2}\right]\end{aligned}$$

$$\begin{aligned}
\lambda_5' = & -\Bigg[(\lambda_1-\lambda_2-A_1)\Bigg(\frac{\beta_{cc}(t)(1-u_1(t))S_cI_c}{N_c^2}+\frac{\beta_{ac}(t)(1-u_2(t))S_cI_a}{N_c^2}\Bigg)\\
& +\lambda_1\rho_c-\lambda_5(\mu+\phi+\rho_c)+\lambda_{10}\phi\Bigg]\\
\lambda_6' = & -\Bigg[(\lambda_7-\lambda_6+A_2)\Bigg(\frac{\beta_{ca}(t)(1-u_3(t))I_c(N_a-S_a)}{N_a^2}\\
& +\frac{\beta_{aa}(t)(1-u_4(t))I_a(N_a-S_a)}{N_a^2}\Bigg)-\lambda_6\mu\Bigg]\\
\lambda_7' = & -\Bigg[(\lambda_6-\lambda_7-A_2)\Bigg(\frac{\beta_{ca}(t)(1-u_3(t))S_aI_c}{N_a^2}\\
& +\frac{\beta_{aa}(t)(1-u_4(t))S_aI_a}{N_a^2}\Bigg)\\
& -\lambda_7(\sigma_a+\mu)+\lambda_8\sigma_a\Bigg]\\
\lambda_8' = & -\Bigg[(\lambda_2+A_1-\lambda_1)\frac{\beta_{ac}(t)(1-u_2(t))S_c}{N_c}\\
& -\lambda_8\big(q_a(1+u_6(t))+\mu+\alpha_{a_1}+\gamma_{a_1}\big)+\lambda_9q_a(1+u_6(t))\\
& +\lambda_{10}\gamma_{a_1}+(\lambda_6-\lambda_7-A_2)\Bigg(\frac{\beta_{ca}(t)(1-u_3(t))S_aI_c}{N_a^2}\\
& -\frac{\beta_{aa}(t)(1-u_4(t))S_a(N_a-I_a)}{N_a^2}\Bigg)\Bigg]\\
\lambda_9' = & -\Bigg[(\lambda_6-\lambda_7-A_2)\Bigg(\frac{\beta_{ca}(t)(1-u_3(t))S_aI_c}{N_a^2}+\frac{\beta_{aa}(t)(1-u_4(t))S_aI_a}{N_a^2}\Bigg)\\
& -\lambda_9\big(\mu+\alpha_{a_2}+\gamma_{a_2}\big)+\lambda_{10}\gamma_{a_2}\Bigg]\\
\lambda_{10}' = & -\Bigg[(\lambda_6-\lambda_7-A_2)\Bigg(\frac{\beta_{ca}(t)(1-u_3(t))S_aI_c}{N_a^2}+\frac{\beta_{aa}(t)(1-u_4(t))S_aI_a}{N_a^2}\Bigg)\\
& +\lambda_6\rho_a-\lambda_{10}(\mu+\rho_a)\Bigg]
\end{aligned}$$

and the transversality conditions $\lambda_i(t_{end})=0, i=1,\ldots,10$.

On the interior of the control set, we can then characterize the optimal control by the optimality condition

$$\begin{aligned}
\frac{\partial H_2}{\partial u_1}\bigg|_{u_1=u_1^*} &= 2B_1u_1^*+\lambda_1\frac{\beta_{cc}(t)S_cI_c}{N_c}-\lambda_2\frac{\beta_{cc}(t)S_cI_c}{N_c}-A_1\frac{\beta_{cc}(t)S_cI_c}{N_c}=0\\
\frac{\partial H_2}{\partial u_2}\bigg|_{u_2=u_2^*} &= 2B_2u_2^*+\lambda_1\frac{\beta_{ac}(t)S_cI_a}{N_c}-\lambda_2\frac{\beta_{ac}(t)S_cI_a}{N_c}-A_1\frac{\beta_{ac}(t)S_cI_a}{N_c}=0,\\
\frac{\partial H_2}{\partial u_3}\bigg|_{u_3=u_3^*} &= 2B_3u_3^*+\lambda_6\frac{\beta_{ca}(t)S_aI_c}{N_a}-\lambda_7\frac{\beta_{ca}(t)S_aI_c}{N_a}-A_2\frac{\beta_{ca}(t)S_aI_c}{N_a}=0,
\end{aligned}$$

$$\left.\frac{\partial H_2}{\partial u_4}\right|_{u_4=u_4^*} = 2B_4u_4^* + \lambda_6\frac{\beta_{aa}(t)S_aI_a}{N_a} - \lambda_7\frac{\beta_{aa}(t)S_aI_a}{N_a} - A_2\frac{\beta_{aa}(t)S_aI_a}{N_a} = 0,$$
$$\left.\frac{\partial H_2}{\partial u_5}\right|_{u_5=u_5^*} = 2B_5u_5^* - \lambda_3q_cI_c + \lambda_4q_cI_c = 0,$$
$$\left.\frac{\partial H_2}{\partial u_6}\right|_{u_6=u_6^*} = 2B_6u_6^* - \lambda_8q_aI_a + \lambda_9q_aI_a = 0.$$

Then we have

$$u_1^* = \min\left\{u_{1_{\max}}, \max\left\{0, \frac{(\lambda_2 + A_1 - \lambda_1)\beta_{cc}(t)S_cI_c}{2N_cB_1}\right\}\right\},$$
$$u_2^* = \min\left\{u_{2_{\max}}, \max\left\{0, \frac{(\lambda_2 + A_1 - \lambda_1)\beta_{ac}(t)S_cI_a}{2N_cB_2}\right\}\right\},$$
$$u_3^* = \min\left\{u_{3_{\max}}, \max\left\{0, \frac{(\lambda_7 + A_2 - \lambda_6)\beta_{ca}(t)S_aI_c}{2N_aB_3}\right\}\right\},$$
$$u_4^* = \min\left\{u_{4_{\max}}, \max\left\{0, \frac{(\lambda_7 + A_2 - \lambda_6)\beta_{aa}(t)S_aI_a}{2N_aB_4}\right\}\right\},$$
$$u_5^* = \min\left\{u_{5_{\max}}, \max\left\{0, \frac{(\lambda_3 - \lambda_4)q_cI_c}{2B_5}\right\}\right\},$$
$$u_6^* = \min\left\{u_{6_{\max}}, \max\left\{0, \frac{(\lambda_8 - \lambda_9)q_aI_a}{2B_6}\right\}\right\}.$$

Appendix D: Proof of Theorem 3

Proof Note that the integrand of the objective functional $J_{c1}(u_1, u_2) + J_{n1}(u_1, u_2)$ is convex on the convex control set U_1, so the existence of an optimal solution $(S_c^*, E_c^*, I_c^*, Q_c^*, R_c^*, S_a^*, E_a^*, I_a^*, Q_a^*, R_a^*)$ with an optimal control (u_1^*, u_2^*) comes from the linearity of the model (16) in the control variables u_i and boundedness by a linear system in the state variables (Fleming and Rishel 2012). □

Appendix E: Fitting with 1-period compared with 2-period

We choose the 1-year-period transmission rates between different populations as follows:

$$\beta_{cc}(t) = \beta_{cc1} - \beta_{cc2}\sin\frac{2\pi(t+\theta)}{365},$$
$$\beta_{ac}(t) = \beta_{ac1} - \beta_{ac2}\sin\frac{2\pi(t+\theta)}{365},$$
$$\beta_{ca}(t) = \beta_{ca1} - \beta_{ca2}\sin\frac{2\pi(t+\theta)}{365},$$

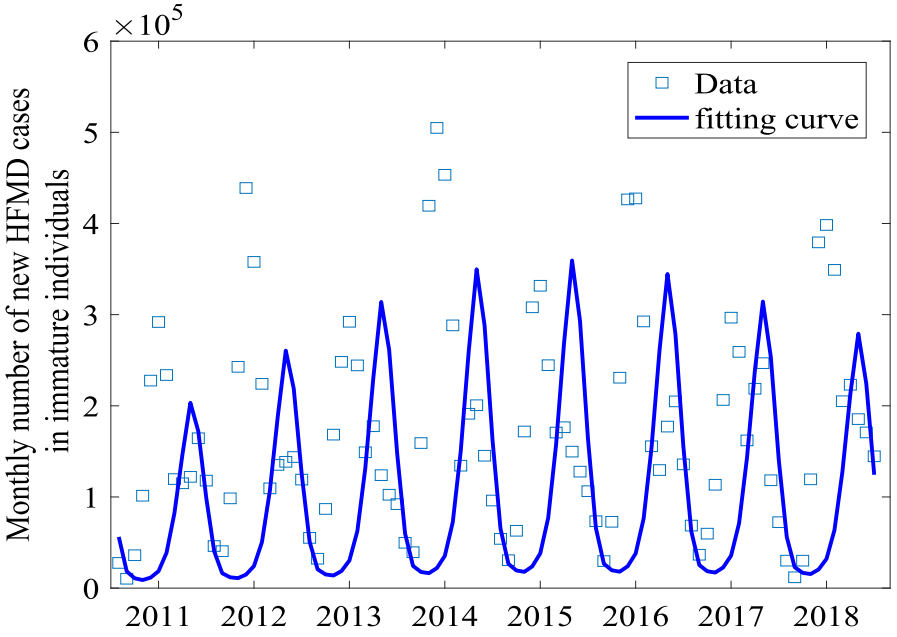

Fig. 13 Fitting result for the data on the monthly number of new HFMD cases in immature individuals in mainland China from January 2011 to December 2018

$$\beta_{aa}(t) = \beta_{aa1} - \beta_{aa2} \sin \frac{2\pi(t+\theta)}{365}.$$

Fitting model (9) to HFMD data is shown in Fig. 13. In Fig. 13, thin blue boxes represent the monthly number of new HFMD cases in mainland China from January 2011 to December 2018, and the best-fitting curve is represented by the dark blue solid curve.

Appendix F: Advantage of optimal controls in different cases

We initially examine the advantage of optimal control in the DBC strategy. In the following, we fix $A_1 = A_2 = 1$, take the baseline value $B_1 = 150000$, $B_2 = 130000$ and consider the following four scenarios:

Case (a_1) $B_j (j = 1, 2)$ reducing to 1/10 of the baseline values;
Case (a_2) $B_j (j = 1, 2)$ expanding to 10 times the baseline values;
Case (a_3) $B_j (j = 1, 2)$ expanding to 100 times the baseline values;
Case (a_4) $B_j (j = 1, 2)$ expanding to 1000 times the baseline values.

The details are shown in Fig. 14 and Tables 5 and 6.

In Fig. 14, the red, green and blue curves represent the effects of no control, constant control and optimal control on the cumulative number of immature HFMD cases. Subplots (a)–(d) illustrate the advantage of the optimal control compared with the constant control and no-control case with the intervention cost coefficients B_1 and B_2 in Cases (a_1)–(a_4), respectively. In Tables 5 and 6, the baseline value represents

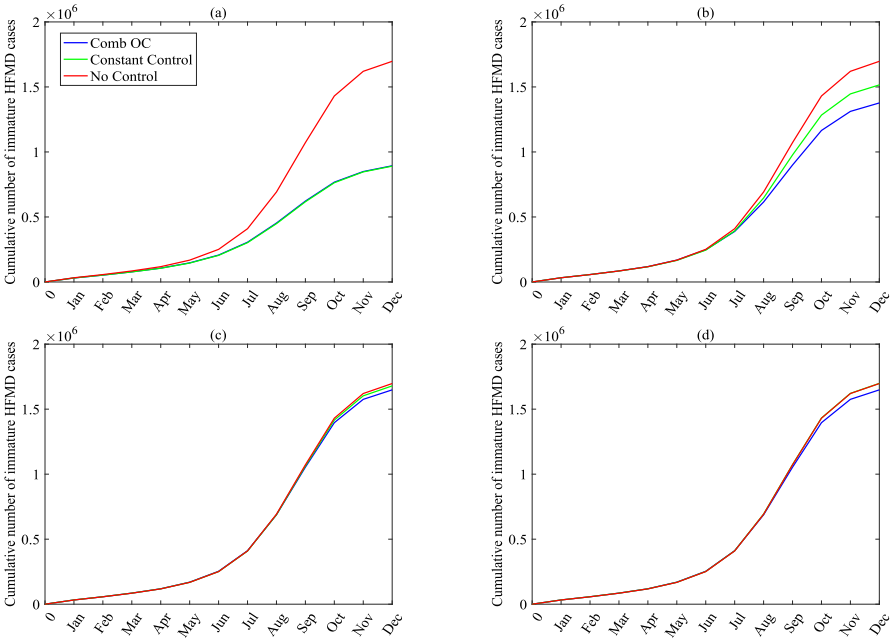

Fig. 14 The advantage of the optimal-control model (16) with the combined objective functional (17) on the cumulative number of immature infected cases in mainland China with different intervention cost coefficients B_1 and B_2 in Cases (a_1)–(a_4)

Table 5 Difference between the optimal control and the constant control and no-control case on the cumulative number of immature infected cases with different intervention cost coefficients in Cases (a_1)–(a_4)

	No control	ConstC	CombOC	diff(I) (%)	diff(II) (%)
Baseline value	1.69706×10^6	9.9091×10^5	9.5023×10^5	−44.01	−4.11
Case (a_1)	1.69706×10^6	8.9084×10^5	8.9381×10^5	−47.33	+0.33
Case (a_2)	1.69706×10^6	1.5158×10^6	1.3769×10^6	−18.87	−9.16
Case (a_3)	1.69706×10^6	1.6788×10^6	1.6484×10^6	−2.87	−1.81
Case (a_4)	1.69706×10^6	1.6983×10^6	1.6915×10^6	−0.33	−0.40

Table 6 Difference between the optimal control and the constant control and no-control case on the total cost with different intervention cost coefficients in Cases (a_1)–(a_4)

	No control	ConstC	CombOC	diff(I) (%)	diff(II) (%)
Baseline value	9.072×10^6	6.8275×10^6	6.2622×10^6	−30.97	−8.28
Case (a_1)	9.072×10^6	5.4416×10^6	5.4240×10^6	−40.21	−0.32
Case (a_2)	9.072×10^6	8.5993×10^6	8.1968×10^6	−9.65	−4.68
Case (a_3)	9.072×10^6	9.0170×10^6	8.9443×10^6	−1.41	−0.81
Case (a_4)	9.072×10^6	9.0749×10^6	9.0480×10^6	−0.26	−0.30

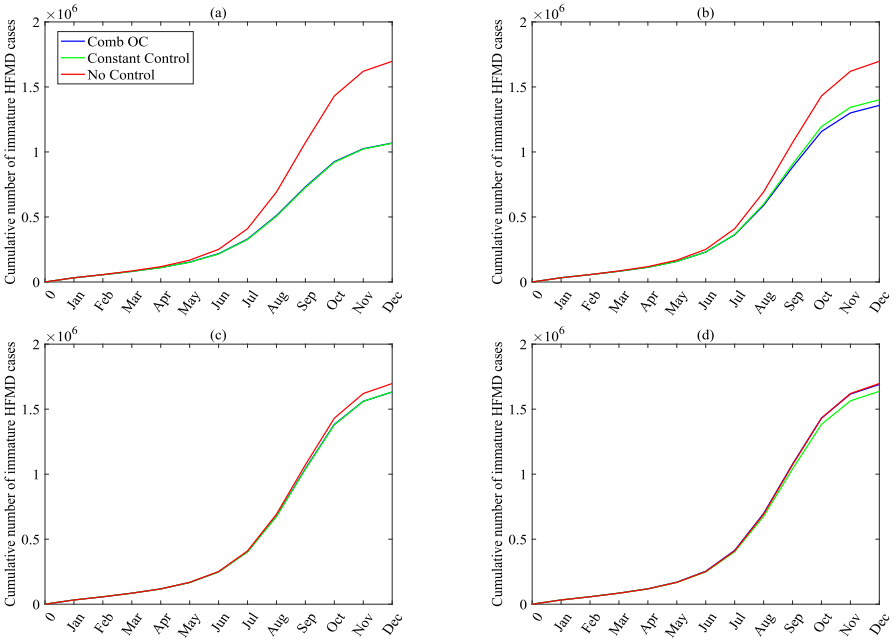

Fig. 15 The advantage of the optimal-control model (19) with the combined objective functional (20) on the cumulative number of immature infected cases in mainland China with different intervention cost coefficients in Cases (b_1)–(b_4)

Table 7 Difference between the optimal control and the constant-control and the no-control cases on the cumulative number of immature infected cases with different intervention cost coefficients in Cases (b_1)–(b_4)

	No control	ConstC	CombOC	diff(I) (%)	diff(II) (%)
Baseline values	1.69706×10^6	1.1528×10^6	1.0957×10^6	−35.44	−4.95
Case (b_1)	1.69706×10^6	1.0666×10^6	1.0682×10^6	−37.15	+0.15
Case (b_2)	1.69706×10^6	1.4012×10^6	1.3581×10^6	−37.06	−3.08
Case (b_3)	1.69706×10^6	1.6333×10^6	1.6317×10^6	−19.97	−0.10
Case (b_4)	1.69706×10^6	1.6373×10^6	1.6898×10^6	−3.85	+3.21

the corresponding values in Table 2. According to Fig. 14 and Tables 5 and 6, we find that variation in the intervention cost coefficients B_1, B_2 leads to differences in the advantages of optimal control over constant control and the no-control case. The optimal control, compared with the no-control case, can achieve the minimum number of infections in mainland China as well as the minimum cost. Compared with the constant-control case, optimal control can also minimise both infections and costs in Cases (a_2)–(a_4); in Case (a_1), the cumulative number of infections and total cost under optimal control are very close to that under constant control.

Table 8 Difference between the optimal control and the constant-control and no-control cases on the total cost with different intervention cost coefficients in Cases (b_1)–(b_4)

	No control	ConstC	CombOC	diff(I) (%)	diff(II) (%)
Baseline values	1.8466×10^6	1.3960×10^6	1.3117×10^6	−28.97	−6.04
Case (b_1)	1.8466×10^6	1.1997×10^6	1.1949×10^6	−35.29	−0.40
Case (b_2)	1.8466×10^6	1.6685×10^6	1.5968×10^6	−13.53	−4.30
Case (b_3)	1.8466×10^6	1.9796×10^6	1.8064×10^6	−2.18	−8.75
Case (b_4)	1.8466×10^6	3.3372×10^6	1.8385×10^6	−0.44	−44.91

Table 9 Epidemiological values corresponding to Fig. 16 with the percentage differences measured from the $A_1 = 5$ and $A_2 = 5$ case

	$A_1 = 5, A_2 = 5$	$A_1 = 1, A_2 = 1$	%difference (%)
Cumulative immature HFMD cases	1.0702×10^6	1.0957×10^6	+2.38
Disease cost $J_{n1}(u_1, u_2)$	5.8999×10^6	1.2064×10^6	−79.55
Intervention cost $J_{c1}(u_1, u_2)$	1.5582×10^5	1.0527×10^5	−32.44
Total cost	6.0557×10^6	1.3117×10^6	−78.34
Total deaths	42	43	+2.38
Time spent at u_{1max}	194	111	−42.78
Time spent at u_{2max}	339	111	−67.26
Time spent at u_{3max}	308	19	−93.83
Time spent at u_{4max}	351	305	−13.11
Time spent at u_{5max}	208	129	−37.98
Time spent at u_{6max}	257	133	−48.25

The other control parameters are in Table 3

Next, we examine the advantage of optimal control in the NIC strategy. We fix $A_1 = A_2 = 1$, take the baseline values $B_1 = 150000$, $B_2 = 130000$, $B_3 = 100000$, $B_4 = 100000$, $B_5 = 150000$, $B_6 = 100000$ and consider the following four scenarios:

Case (b_1) $B_j (j = 1, \ldots, 6)$ reducing to 1/10 of the baseline values;
Case (b_2) $B_j (j = 1, \ldots, 6)$ expanding to 10 times the baseline values;
Case (b_3) $B_j (j = 1, \ldots, 6)$ expanding to 100 times the baseline values;
Case (b_4) $B_j (j = 1, \ldots, 6)$ expanding to 1000 times the baseline values.

The effect of the optimal control with different intervention cost coefficients in controlling the cumulative number of immature infections is shown in Fig. 15 and Tables 7 and 8.

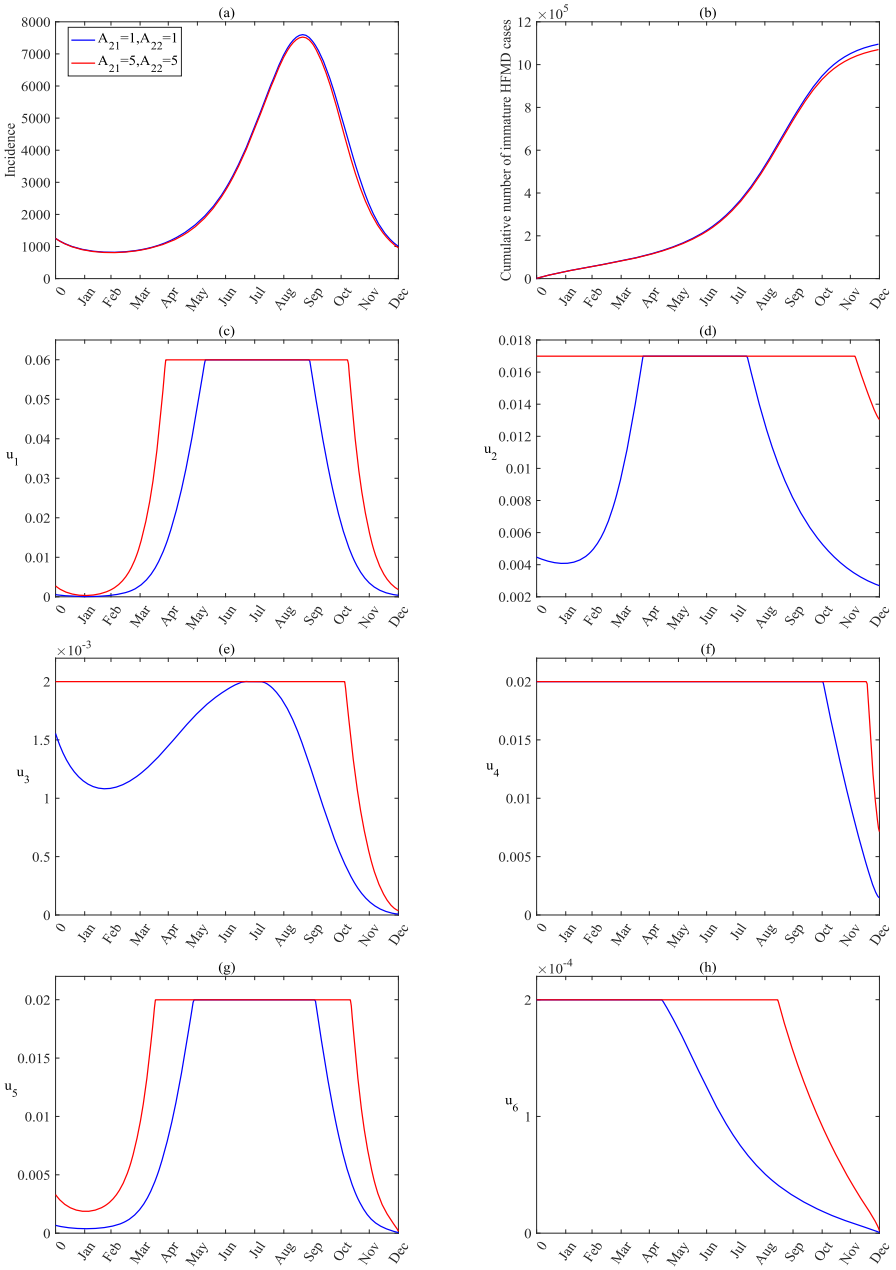

Fig. 16 Optimal control, incidence and cumulative number of immature HFMD cases in 2018 for the optimal model (19) with the combined objective functional (20) for different A_1, A_2 values, corresponding to the results in Table 9

In Fig. 15, the red, green and blue curves represent the effects of no control, constant control and optimal control on the cumulative number of immature HFMD cases in 2018. In Tables 7 and 8, the baseline value represents the corresponding values in Table 3. According to Fig. 15 and Tables 7 and 8, we also find that the optimal control, compared with the no-control case, can achieve the minimum number of infections in mainland China as well as the minimum cost. Compared with the constant-control case, optimal control can also achieve the minimum infections and total cost in Cases (b_2)–(b_3); in Cases (b_1), the cumulative number of infections and total cost under optimal control are very close to that under constant control; in Case (b_4), the cumulative number of infections under optimal control is slightly larger than that under constant control, but the total cost under optimal control is significantly lower than that under constant control. The results demonstrate that optimal control, compared with the constant-control or no-control cases, is still the most advantageous by reducing infections and cost.

In the following, we will investigate the influence of variation in the per-capita, daily productivity loss on the spread of the disease. To this end, we simulated the NIC strategy by setting the unit cost A_1 for each new case to either 5 or 1 and the unit cost A_2 to either 5 or 1. The results were shown in Table 9 and Fig. 16. The parameters in Fig. 16 and Table 9 are the same as in Tables 1 and 3, with the time horizon as in Table 2. If the unit cost of the disease is underestimated, simulations of the NIC strategy indicate that the optimal strategy entails 2.38% more cases and lives lost, although it leads to a 78.34% reduction in the total cost.

Acknowledgements The authors are grateful to three anonymous reviewers, whose comments greatly improved the manuscript. This research was funded by the National Natural Science Foundation of China (Grant Number: 12271431, 12371404) and special scientific research project of emergency public health security of education department of Shaanxi province (Grant Number: 20JG002). SS? was supported by an NSERC Discovery Grant. For citation purposes, please note that the question mark in "Smith?" is part of her name.

Declarations

Conflict of interest The authors declare no conflict of interest.

References

McMinn P, Lindsay K, Perera D et al (2001) Phylogenetic analysis of enterovirus 71 strains isolated during linked epidemics in Malaysia, Singapore, and Western Australia. J Virol 75(16):7732–7738

Chen Y, Chen Y, Tao R (2010) Interpretation of hand-foot-mouth disease diagnosis and treatment guidelines (2010 edition). World Infect, 30(3):104–108

Zhao J, Jiang F, Zhong L et al (2016) Age patterns and transmission characteristics of hand, foot and mouth disease in China. BMC Infect Dis 16(1):691

Chinese people's net. Law of the People's Republic of China on the Prevention and Control of Infectious Diseases. http://www.npc.gov.cn/npc/c191/c12481/search/index.html?allKeywords=Law of the People's Republic of China on the Prevention and Control of Infectious Diseases

Mathes EF, Oza V, Frieden IJ et al (2013) "Eczema coxsackium" and unusual cutaneous findings in an enterovirus outbreak. Pediatrics 132(1):e149–e157

Yang S, Wu J, Ding C et al (2017) Epidemiological features of and changes in incidence of infectious diseases in China in the first decade after the SARS outbreak: an observational trend study. Lancet Infect Dis 17(7):716–725

World Health Organization. Hand Foot and Mouth Disease in Vietnam. https://www.who.int/vietnam/news/detail/07-09-2011-hand-foot-and-mouth-disease-in-viet-nam
Chinese Center for Disease Control and Prevention (China CDC). Public health science data: Hand, Foot and Mouth disease. https://www.chinacdc.cn
Xing W, Liao Q, Viboud C et al (2014) Hand, foot, and mouth disease in China, 2008–12: an epidemiological study. Lancet Infect Dis 14(4):308–318
Zhao J, Hu X (2019) The complex transmission seasonality of hand, foot, and mouth disease and its driving factors. BMC Infect Dis 19(1):1–12
Xiao X, Liao Q, Kenward MG et al (2016) Comparisons between mild and severe cases of hand, foot and mouth disease in temporal trends: a comparative time series study from mainland China. BMC Public Health 16(1):1109
Wu C, Gao L (2020) Epidemiological characteristics of hand, foot and mouth disease in Xiangshan County, Ningbo City, 2009–2019. Modern Pract Med 32(12):1497–1501
Zhang Y, Liu Q, Zheng F et al (2018) Epidemiological characteristics of HFMD clusters in Fengxian District, Shanghai from 2012 to 2015. J Trop Med 18(2):252–255
Liu D, Leung K, Jit M et al (2020) Cost-effectiveness of bivalent versus monovalent vaccines against hand, foot and mouth disease. Clin Microbiol Infec 26(3):373–380
Li Y, Wang L, Pang L et al (2016) The data fitting and optimal control of a hand, foot and mouth disease (HFMD) model with stage structure. App Math Comput 276:61–74
Zhao H, Shi L, Wang J et al (2021) A stage structure HFMD model with temperature-dependent latent period. Appl Math Model 93:745–761
Li C, Mao J, Wu Y et al (2023) Combined impacts of environmental and socioeconomic covariates on HFMD risk in China: A spatiotemporal heterogeneous perspective. Plos Neglect Trop 17(5):e0011286
Qu D, Song X, Liu X (2018) Investigation of enterovirus carrying in close contacts of children with hand, foot and mouth disease. Henan Prevent Med 29(06):425–427
Wu Q, Fu X, Jiang L et al (2017) Prevalence of enteroviruses in healthy populations and excretion of pathogens in patients with hand, foot, and mouth disease in a highly endemic area of southwest China. Plos One 12(7):e0181234
Liu J (2011) Threshold dynamics for a HFMD epidemic model with periodic transmission rate. Nonlinear Dynam 64:89–95
Ma Y, Liu M, Hou Q et al (2013) Modelling seasonal HFMD with the recessive infection in Shandong. China. Math Biosci Eng 10(4):1159–1171
Wang J, Xiao Y, Peng Z (2016) Modelling seasonal HFMD infections with the effects of contaminated environments in mainland China. Appl Math Comput 274:615–627
Wang J, Xiao Y, Cheke R (2019) Modelling the effects of contaminated environments in mainland China on seasonal HFMD infections and the potential benefit of a pulse vaccination strategy. Discrete Cont Dyn-B 24(11):5849–5870
Shi L, Zhao H, Wu D (2020) Modeling periodic HFMD with the effect of vaccination in mainland China. Complexity 2020:8763126
Dai C, Wang W, Li Y et al (2019) Epidemics and underlying factors of multiple-peak pattern on hand, foot and mouth disease in Wenzhou. China. Math Biosci Eng 16(4):2168–2188
Ding Z, Li Y, Cai Y et al (2020) Optimal control strategies of HFMD in Wenzhou. China. Complexity 2020:5902698
Tan H, Cao H (2018) The dynamics and optimal control of a hand-foot-mouth disease model. Comput Math Method M 2018:9254794
Wongvanich N, Tang IM, Dubois MA et al (2021) Mathematical modeling and optimal control of the hand foot mouth disease affected by regional residency in Thailand. Mathematics 9(22):2863
Yang J, Chen Y, Zhang F (2013) Stability analysis and optimal control of a hand-foot-mouth disease (HFMD) model. J Appl Math Comput 41:99–117
Shi R, Lu T (2020) Dynamic analysis and optimal control of a fractional order model for hand-foot-mouth disease. J Appl Math Comput 64(1–2):565–590
Tan C, Li S, Li Y et al (2023) Dynamic modeling and data fitting of climatic and environmental factors and people's behavior factors on hand, foot, and mouth disease (HFMD) in Shanghai, China. Heliyon 9(8):e18212
Jing SL, Huo HF, Xiang H (2020) Modeling the Effects of Meteorological Factors and Unreported Cases on Seasonal Influenza Outbreaks in Gansu Province, China. Bulletin of Mathematical Biology 82(6):73
Zhao XQ (2003) Dynamical systems in population biology. Springer, New York

Huang TZ, Yang CS (2007) Special matrix analysis and application. Science Press, Beijing
Zhang F, Zhao XQ (2007) A periodic epidemic model in a patchy environment. J Math Anal Appl 325(1):496–516
Wang W, Zhao XQ (2008) Threshold dynamics for compartmental epidemic models in periodic environments. J Dyn Differ Equ 20:699–717
Hale JK (2010) Asymptotic behavior of dissipative systems. American Mathematical Soc
National Bureau of Statistics of China. National data. http://data.stats.gov.cn
Johnson ML, Faunt LM (1992) Parameter estimation by least-squares methods. Academic Press 210:1–37
Pontryagin LS (1985) The mathematical theory of optimal processes and differential games. Trudy Mat. Inst. Steklov 169:119–158
Pontryagin LS, Boltyanskii VG, Gamkrelize RV, Mishchenko EF (1962) The Mathematical Theory of Optimal Processes. Wiley, New York
Fleming WH, Rishel RW (2012) Deterministic and stochastic optimal control. Springer Science & Business Media
Igoe M, Casagrandi R, Gatto M et al (2023) Reframing optimal control problems for infectious disease management in low-income countries. B Math Biol 85(4):31
Lenhart S, Workman JT (2007) Optimal control applied to biological models. CRC Press